

Modeling adsorption of organic compounds on activated carbon

A multivariate approach

by

Jufang Wu

Akademisk avhandling

Som med tillstånd av rektorsämbetet vid Umeå universitet för erhållande
av Filosofie Doktorsexamen vid Teknisk-naturvetenskapliga fakulteten I
Umeå, framlägges till offentlig granskning vid Kemiska Institutionen,
hörsal KB3A9 i KBC, fredagen den 24 september 2004, kl. 13.00.

Fakultetsopponent: Professor Fritz Stoeckli, L'Institut de Chimie de
l'Université de Neuchâtel, Neuchâtel, SCHWEIZ.

Front cover:
Adsorption action on a particle of activated carbon

ISBN: 91-7305-697-9
Copyright © 2004 by Jufang Wu
Printed in Sweden by Solfjädern Offset AB, Umeå 2004

Title Modeling adsorption of organic compounds on activated carbon—A multivariate approach

Author Jufang Wu, Analytical Chemistry, Department of Chemistry, Umeå University, SE-901 87 Umeå, Sweden and Swedish Defence Research Agency, Division of NBC Defence, SE-901 82 Umeå, Sweden

Abstract: Activated carbon is an adsorbent that is commonly used for removing organic contaminants from air due to its abundant pores and large internal surface area. This thesis is concerned with the static adsorption capacity and adsorption kinetics for single and binary organic compounds on different types of activated carbon. These are important parameters for the design of filters and for the estimation of filter service life. Existing predictive models for adsorption capacity and kinetics are based on fundamental “hard” knowledge of adsorption mechanisms. These models have several drawbacks, especially in complex situations, and extensive experimental data are often needed as inputs. In this work we present a systematic approach that can contribute to the further development of predictive models, especially for complex situations. The approach is based on Multivariate Data Analysis (MVDA), which is ideally suited for the development of soft models without incorporating any assumptions about the mathematical form or fundamental physical principles involved.

Adsorption capacity and adsorption kinetics depend on the properties of the carbon and the adsorbate as well as experimental conditions. Therefore, to make general statements regarding adsorption capacity and kinetics it is important for the resulting models to be representative of the conditions they will simulate. Accordingly, the first step in the investigations underlying this thesis was to select a minimum number of representative and chemically diverse organic compounds. The next steps were to study the dependence of the derived affinity coefficient, β , in the Dubinin-Radushkevich equation on properties of organic compounds and to establish a new, improved model. This new model demonstrates the importance of adding descriptors for the specific interaction with the carbon surface to the size and shape descriptors. The adsorption capacities of the same eight organic compounds at low relative pressures were correlated with compound properties. It was found that different compound properties are important in the various stages of adsorption, reflecting the fact that different mechanisms are involved. Ideal adsorbed solution theory (IAST) in combination with the Freundlich equation was developed to predict the adsorption capacities of binary organic compound mixtures. A new model was proposed for predicting the rate coefficient of the Wheeler-Jonas equation which is valid for breakthrough ratios up to 20%. Finally, it was shown that the Wheeler-Jonas equation can be adapted to describe the breakthrough curves of binary mixtures. New models were proposed for predicting its parameters, the adsorption rate coefficients, and the adsorption capacities for both components of the binary mixture. Thus, multivariate data analysis can not only be used to assist in the understanding of adsorption mechanisms, but also contribute to the development of predictive models of adsorption capacity and breakthrough time for single and binary organic compounds.

Keywords: Activated carbon, Adsorption, Adsorption capacity, Adsorption rate, PCA, PLS, Binary mixtures, Dubinin-Rauskevich, Wheeler-Jonas



To my dearest parents

This thesis is based on the following papers referred to by their Roman numerals

I. Jufang Wu, Marianne E. Strömqvist, Ola Claesson, Ingrid E. Fängmark, Lars-Gunnar Hammarström

A systematic approach for modeling the affinity coefficient in the Dubinin-Radushkevich equation

Carbon 40:2587-2596 (2002)

II Jufang Wu, Lars-Gunnar Hammarström, Ola Claesson, Ingrid E. Fängmark

Modeling the influence of physico-chemical properties of volatile organic compounds on activated carbon adsorption capacity

Carbon 41:1322-1325 (2003)

III Jufang Wu, Zili Xie, Kunmin Guo, Ola Claesson

Measurement and prediction of the adsorption of binary mixtures of organic vapors on activated carbon

Adsorption Science & Technology 19:737-749 (2001)

IV Jufang Wu, Ola Claesson, Ingrid Fängmark, Lars-Gunnar Hammarström

A systematic investigation of the overall rate coefficient in the Wheeler-Jonas equation for adsorption on dry activated carbons

Submitted, 2004

V Jufang Wu, Ola Claesson, Ingrid Fängmark, Lars-Gunnar Hammarström

Service life of activated carbon beds exposed to binary organic vapor mixtures

Manuscript.

Published papers are reproduced with kind permission from Elsevier (for *Carbon*) and Multi Science Publishing Co Ltd (for *Adsorption Science & Technology*).

LIST OF ABBREVIATIONS

AC	Activated Carbon
CV	Cross Validation
DR	Dubinin-Radushkevich equation
GC	Gas Chromatography
IAST	Ideal Adsorbed Solution Theory
MPD	Myers-Prausnitz and Dubinin method
MS	Mass Spectrometry
MTZ	Mass Transfer Zone
MVDA	Multivariate Data Analysis
PCA	Principal Component Analysis
PC	Principal Component
PLS	Partial Least Squares Projection to Latent Structures
QSAfR	Quantitative Structure Affinity Relationship
Q^2	Cross validated explained variance
R^2	Explained variance
RMSEE	Root Mean Square Error of Estimation
RMSEP	Root Mean Square Error of Prediction
VOC	Volatile Organic Compound
W-J	Wheeler-Jonas equation

TABLE OF CONTENTS

1 INTRODUCTION	1
2 OVERVIEW OF THE THESIS	3
3 BACKGROUND.....	5
3.1 Activated carbon	5
3.2 Adsorption	7
3.3 Adsorption capacity, adsorption rate, and existing single-component predictive models.....	8
3.3.1 Adsorption capacity.....	8
3.3.2 Dynamic adsorption in activated carbon beds.....	12
3.3.3 Existing models for the adsorption rate coefficient.....	17
3.4 Multi-component adsorption	18
4 MATERIALS AND METHODS	21
4.1 Statistical experimental design.....	21
4.2 Selection of adsorbates.....	22
4.2.1 Property descriptors of compounds	22
4.2.2 Principal component analysis (PCA)	22
4.2.3 Selection of the training set as single adsorbates	24
4.2.4 Selection of binary adsorbate systems	26
4.3 The activated carbons used in this study.....	27
4.4 Experimental methods	27
4.4.1 Adsorption equilibrium measurements	27
4.4.2 Breakthrough measurements	28
4.5 Modeling.....	30
4.5.1 Partial least squares projection to latent structures (PLS)	30
4.5.2 Model assessment and validation	32
5 RESULTS AND DISCUSSION	34

5.1 Modeling the affinity coefficient (Paper I)	34
5.2 The influence of compound properties on adsorption capacity (Paper II)	35
5.3 Adsorption equilibria of binary systems (Paper III)	37
5.4 Modeling the adsorption rate coefficient (Paper IV)	38
5.5 Prediction of the service life of carbon beds in the presence of binary adsorbates (Paper V)	40
6 CONCLUSIONS	44
7 FUTURE WORK	46
8 ACKNOWLEDGEMENTS	47
9 REFERENCES	48
APPENDICES I -III	56

1 INTRODUCTION

Many volatile organic compounds (VOCs) are toxic, posing a high risk to human health as a result of their widespread use and occurrence in workplace environments. Reducing the amount of organic vapors in ambient air is, therefore, an important task. Activated carbons are the most versatile and frequently used adsorbents, and fixed beds of activated carbon, in the form of canisters or filters, are widely used for purifying contaminated air. Its large internal surface area and pore volume, its ability to adsorb most organic vapors and low cost make activated carbon one of the most practical adsorbents (Prakash et al. 1994).

Activated carbon beds eventually become exhausted after continuous exposure to air contaminated with organic vapors. The time at which an organic vapor of a defined concentration is able to penetrate the bed is known as the breakthrough time of the adsorbate. In practical situations, a key factor is the service life of the filter. This is defined as the time at which the concentration of the compound penetrating the filter reaches an unacceptable level. An accurate estimate of this service life is of great importance to both users and manufacturers. A predictive model for filter performance would reduce the need for time consuming filter tests, aid in the design of filters with optimized performance and provide knowledge of the service life of military filters exposed to conditions and chemicals encountered in civilian situations.

In order to predict breakthrough times, knowledge of both the adsorption equilibrium capacity and the adsorption kinetics is required. A number of adsorption models have been developed for predicting the breakthrough times of organic vapors in filters containing activated carbon (Ackley, 1985). The complexity of the adsorption process, however, makes it necessary to use simplifying assumptions in deriving the models. Furthermore, these models have been derived from the performance of a limited number of compounds with limited structural variation. The existing models therefore suffer from a number of drawbacks, especially for complex situations, such as the adsorption of multi-component mixtures.

This thesis describes the results of applying a systematic approach to the development of predictive models for the adsorption of organic compounds. The approach is based on a statistical tool known as Multivariate Data Analysis (MVDA; Wold et al. 1984). MVDA is a mathematical technique for building global models of complex systems. Its strength lies in the simultaneous treatment of many variables and the resulting information on the complex interplay between different factors. To maximize the information obtained from a minimum number of experiments, the study also involved the use of experimental design for training a global model.

Introduction

The aims of the work underlying this thesis were:

- to increase the knowledge of fundamental aspects of adsorption
- to determine the relationship between adsorbate properties and the corresponding adsorption capacity and kinetic rate constant
- to develop a predictive model for filter performance in the presence of binary mixtures of organic compounds.

2 OVERVIEW OF THE THESIS

The overall aim of this work was to explore the merits of applying a systematic approach to the development of predictive models for the service life of fixed activated carbon beds exposed to mixtures of organic compounds.

This systematic approach consists of the following steps:

1. Selection of a set of training data through:
 - a) characterization of adsorbate properties using a multitude of descriptor variables.
 - b) calculation of principal properties.
 - c) factorial design in the principal properties
2. Performance tests
3. Structure-affinity modeling.
4. Validation of the model.

The Wheeler-Jonas equation is frequently used to evaluate the breakthrough time of organic compounds in activated carbon beds. To use this equation for predicting service lives, two parameters need to be known: the adsorption capacity W_e and adsorption rate coefficient k_r .

Paper I considers ways for improving accuracy in predicting W_e . The dependence of the affinity coefficient, β , on adsorbate properties is examined and a new model for deriving β is developed.

In Paper II, adsorption capacities at low relative pressures are correlated with properties of organic compounds, thereby increasing understanding of the mechanisms involved in the different stages of the adsorption process.

Paper IV is an investigation of the factors influencing the rate coefficient k_r , including adsorbate and carbon properties, inlet concentration and flow velocities. A new model for determining k_r is proposed.

Paper III describes a procedure for predicting the adsorption capacities of binary mixtures using the ideal adsorbed solution theory (IAST).

When binary mixtures are being adsorbed, W_e and k_r for each compound in the mixture may differ from the corresponding values for the adsorption of the individual compounds. In Paper V these changes in W_e and k_r are modeled on the basis of the physico-chemical properties of both compounds, making it possible to derive W_e and k_r for each compound in the binary mixture from W_e and k_r for the single compounds. Based on this, the service

Overview of the thesis

lives of activated carbon beds exposed to binary mixtures of organic compounds are predicted.

Schematically, the five papers are related as follows:

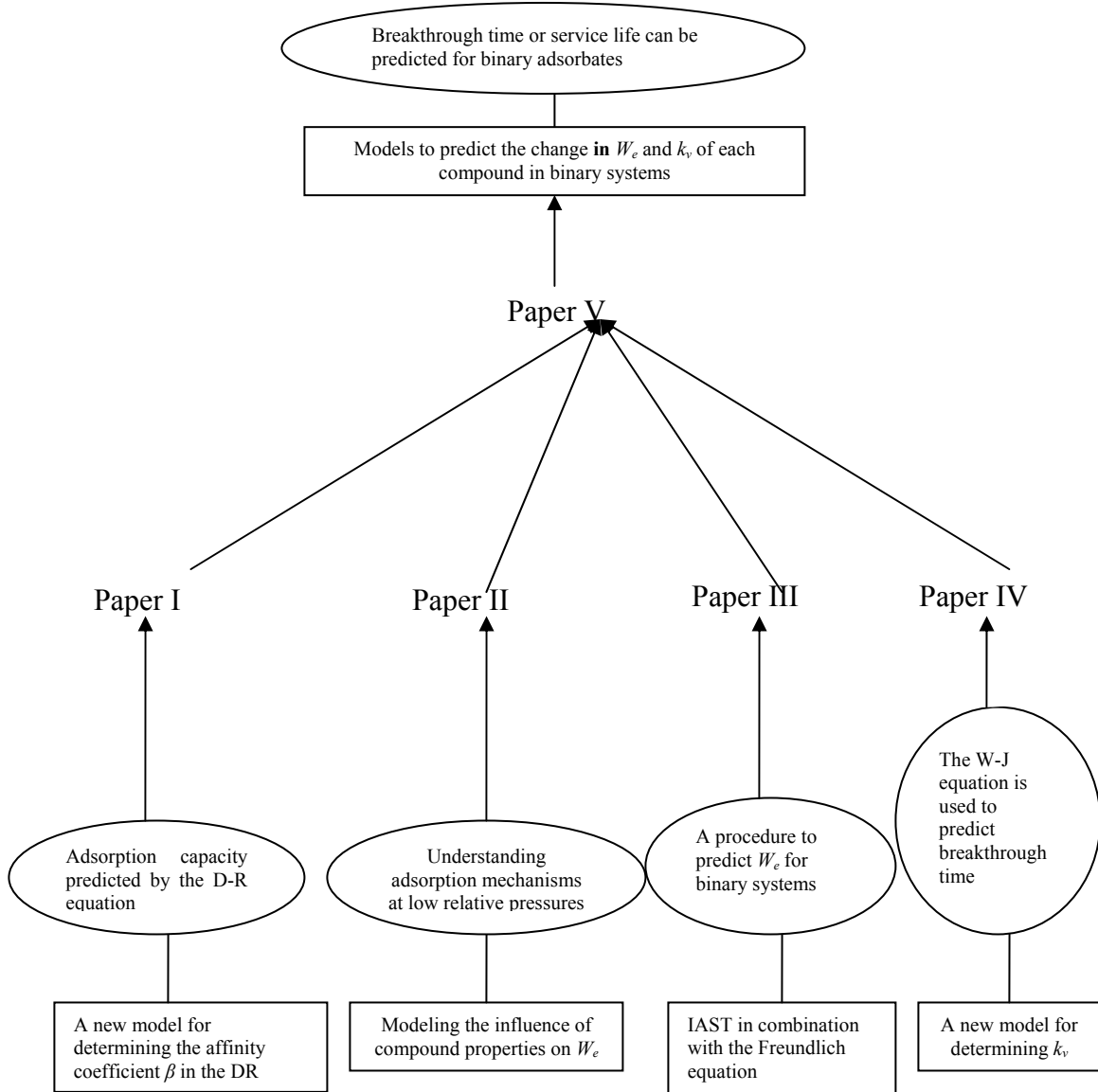
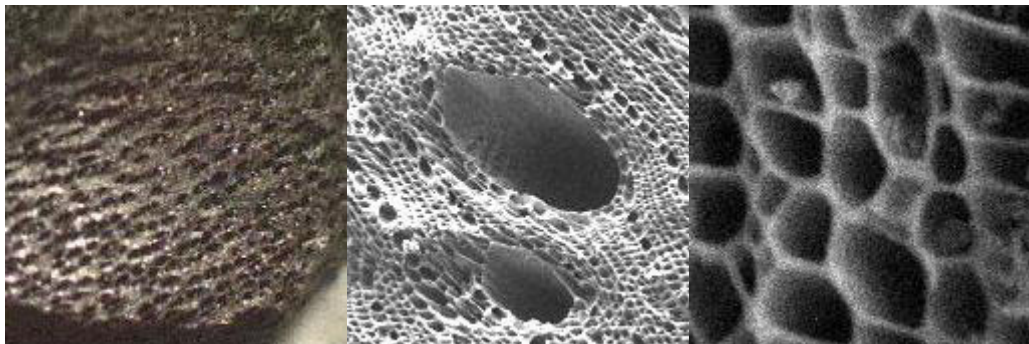


Fig. 2.1: Overview of the papers included in the thesis.

3 BACKGROUND

3.1 Activated carbon

Activated carbon is a solid, porous, black carbonaceous material, see Fig.3.1. It is distinguished from elemental carbon by the absence of both impurities and an oxidized surface (Mattson and Mark, 1971). It can be prepared from a large number of sources such as coconut, wood, peat, coal, tar, sawdust, and cellulose residues (Lambotte, 1942). Any carbon source can be converted into activated carbon via a number of methods. Usually, the process is divided into carbonization and activation. During carbonization most of the non-carbon elements are removed in gaseous form by the pyrolytic decomposition of the source material. The porous structure is mainly developed during activation by means of an activation agent that reacts with the carbon. Such agents may include synthetic acids, bases, and other substances in a stream of activating gases such as steam (H_2O), nitrogen (N_2) or carbon dioxide (CO_2).



*Fig.3.1: Activated carbon: surface and pores – scanning electron microscope image.
Magnification increases from left to right. (Courtesy of Roplex Engineering Ltd.).*

Activated carbon has an extraordinarily large surface area and pore volume, making it suitable for a wide range of applications. It can be used as a decolorizing agent, a taste and odor removing agent or as a purification agent in food processing. One major use of activated carbon is in water purification, including the production of potable water and the treatment of waste and ground waters. Water treatment accounts for approximately half of the total use of activated carbon in the US (Baker et al., 1992). There are also a number of applications related to purification processes in the clothing, textile, automobile, cosmetics, and pharmaceutical industries. The hundreds of other uses include its utilization as an adsorbent in gas mask filters and as a pollution control material in a range of filters (Ashford, 1994). Activated carbon is the major adsorbent used in canisters and filters because it adsorbs a large variety of organic compounds, it is cheap, and it can

Background

be reused if the adsorbed substances are removed. This regeneration is often achieved by heating (Battelle, 1970).

Activated carbon is produced in various forms, including powders, cylindrical extrudates, spherical beads, granules and fibers. The slit-shaped model in Fig.3.2 represents the microstructure of activated carbon (Stoeckli, 1990).



Fig.3.2: A schematic representation of the structure of activated carbon. Adapted from Stoeckli (1990) (Courtesy of Elsevier).

The most important property of activated carbon, the property that determines its usage, is the pore structure. The total number of pores, their shape and size determine the adsorption capacity and even the dynamic adsorption rate of the activated carbon. IUPAC classifies pores as follows (Rodriguez-Reinoso and Linares-Solano, 1989):

macropores: $d_0 > 50\text{nm}$

mesopores: $2 \leq d_0 \leq 50\text{nm}$

micropores: $d_0 < 2\text{nm}$

ultramicropores: $d_0 < 0.7\text{nm}$

supermicropores: $0.7 < d_0 < 2\text{nm}$

where d_0 is the pore width for slit type pores or the pore diameter for cylindrical pores.

Fig.3.3 illustrates the different types of pores.

Background

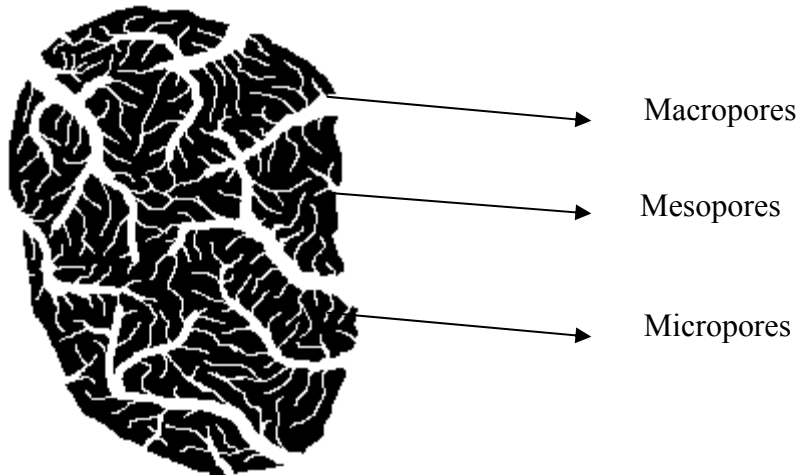


Fig.3.3: Schematic representation of the different types of pores in an activated carbon particle.

The macropores act as transport pathways, through which the adsorptive molecules travel to the mesopores, from where they finally enter the micropores. The micropores usually constitute the largest proportion of the internal surface of the activated carbon and contribute most to the total pore volume. Most of the adsorption of gaseous adsorptives takes place within these micropores, where the attractive forces are enhanced and the pores are filled at low relative pressures. Thus, the total pore volume and the pore size distribution determine the adsorption capacity.

The dynamics of adsorption in a packed activated carbon bed are influenced by the shape and size of the activated carbon particles and their effect on the flow characteristics. The smaller an activated carbon particle is, the better the access to its surface area and the faster the rate of adsorption. For spherical beads, the diameter can be measured easily. For cylindrical extrudates, an equivalent spherical diameter, d_{eqv} , can be calculated from the radius and length of the extrudate. However, for particles of irregular shape and a wide size distribution, it is difficult to derive d_{eqv} . In such cases particle sizes derived from sieve analyses can be useful parameters for determining adsorption rate.

3.2 Adsorption

Adsorption is defined as the enrichment of material or increase in the density of the fluid in the vicinity of an interface with a solid (the adsorbent) (Sing et al., 1985). It may be classified as chemisorption or physisorption, depending on the nature of the interactive forces. In chemisorption the transfer of electrons is significant and equivalent to the formation of a chemical bond between the sorbate and the solid surface. In physisorption the interactive forces are relatively weak.

Background

This study is restricted to mechanisms involved in the physisorption of organic vapors onto activated carbon. It is likely, however, that the technique used also has some potential with respect to chemisorption. Physisorption occurs whenever an adsorbable fluid (the adsorptive) is brought into contact with the surface of the adsorbent. The intermolecular forces involved are of the same kind as those responsible for the imperfection of real gases and the condensation of vapors (Kenny et al., 1993; Kaneko, 1997). In addition to attractive dispersion forces and short range repulsive forces, the so called van der Waals forces, dipole–dipole, induced dipole–induced dipole and dipole–induced dipole interactions all occur as a result of particular geometric and electronic properties of the adsorbent and adsorptive. The molecules are adsorbed when their potential energy is at a minimum.

Adsorption proceeds through the following steps:

- 1) Mass transfer – adsorptive molecules transfer to the exterior of the activated carbon granules;
- 2) Intragranular diffusion – molecules move into the carbon pores;
- 3) Physical adsorption.

Thus, adsorption depends on (Cheremisionoff and Morresi, 1978):

- a) the physical and chemical characteristics of the adsorbent (activated carbon);
- b) the physical and chemical characteristics of the adsorbate (organic vapors);
- c) the concentration of the adsorbate
- d) experimental conditions, such as temperature, air flow velocity and relative humidity.

3.3 Adsorption capacity, adsorption rate, and existing single-component predictive models

3.3.1 Adsorption capacity

Laboratory evaluation of the adsorption isotherm* and the adsorption capacity# is time consuming and may be affected by toxicity or the availability of the adsorbate. For such difficult cases, a model that can predict the adsorption capacity, making testing unnecessary, would be highly desirable. A number of such models have been proposed for the adsorption isotherm: the Freundlich isotherm equation (Freundlich 1926); the Langmuir isotherm (Langmuir 1916 and 1918); BET-theory (Brunauer, Emmett and Teller, 1938); the Hacskaylo and LeVan equation (Hacskaylo and LeVan 1985); the Dubinin-Raduskevish (DR) equation (Dubinin 1966); and a modification of the DR equation developed by Stoeckli (Stoeckli 1977, 1979).

Background

Among the existing predictive equations, the DR equation has been the most widely used to predict organic vapor adsorption onto activated carbon (Wood 1992, Stoeckli 1998). It has several advantages:

- a) there is a good data fit over a wide concentration range
- b) temperature is included as a parameter
- c) it is built around physical parameters
- d) it is easy to apply.

Dubinin postulated that the amount of vapor adsorbed (W) by an activated carbon source, at a relative pressure (P/P_s), is a function of the thermodynamic potential (A), with A expressed as

$$A = RT \ln\left(\frac{P_s}{P}\right) \quad (3-1)$$

where R is the universal gas constant, T is the absolute temperature, P_s is the saturated vapor pressure at temperature T , and P is the partial pressure of the adsorbate.

By examining the adsorption of simple organic compounds, such as benzene, Dubinin concluded that the function was Gaussian. This led to the classical expression of Dubinin and Radushkevich (the D-R equation) (Dubinin, 1975):

$$W = W_0 * \exp\left[-\left(\frac{A}{\beta E_0}\right)^2\right] \quad (3-2)$$

where W_0 is the maximum amount adsorbed, E_0 is the characteristic adsorption energy for a reference vapor on a specific adsorbent. The parameter β is called the affinity coefficient or similarity coefficient, and expresses the ratio of the characteristic free energies of adsorption for the test and reference vapors (Urano et al., 1982; Stoeckli and Morel 1980). Benzene is, by convention, used as the reference compound for carbonaceous materials, and is, by definition, given the value $\beta = 1$.

* The adsorption isotherm is a graphical representation of the adsorption capacity versus the equilibrium gas phase concentration.

The adsorption capacity is the amount of the molecule adsorbed (the adsorbate) per unit mass of the adsorbent at a given gas-phase concentration under equilibrium conditions. It corresponds to one point on the adsorption isotherm.

Background

β is only related to the properties of the adsorptive, and is independent of the adsorbent (Dubinin, 1975). The value of β has a significant influence on adsorption capacities calculated using the DR equation. The influence is most pronounced at low relative pressures, as shown by Fig.3.4.

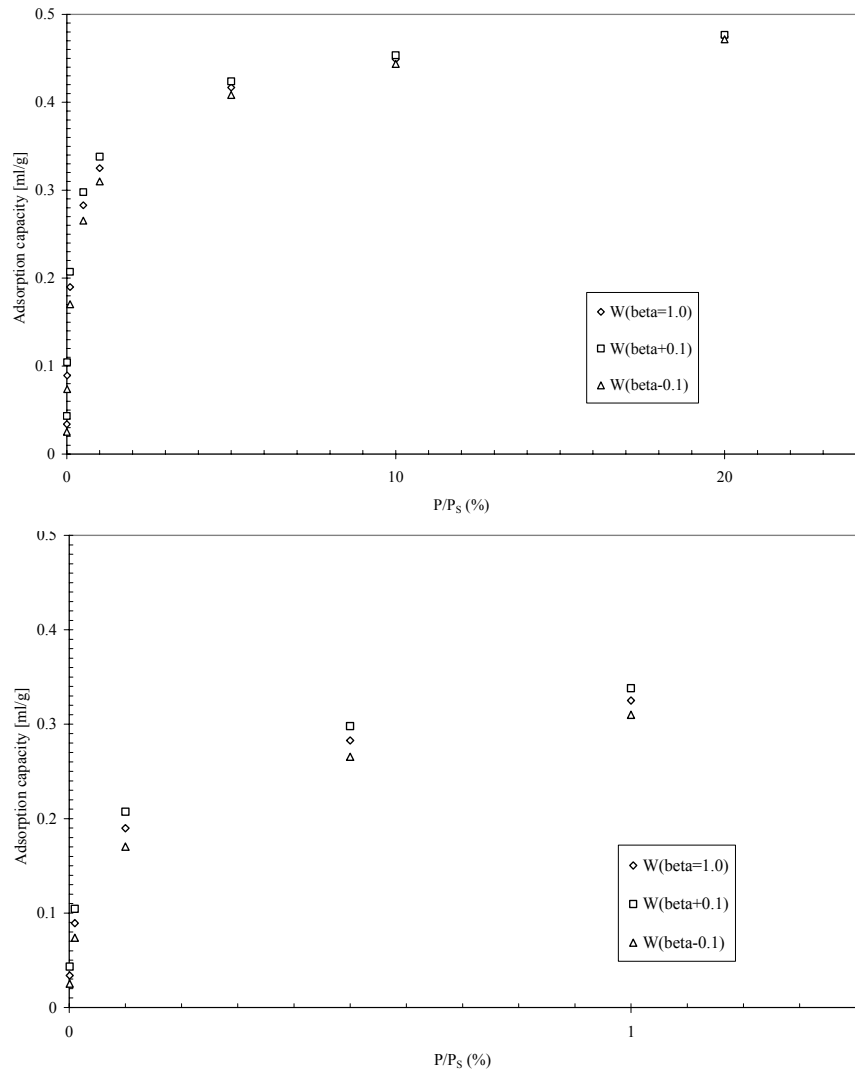


Fig.3.4: The influence of β on adsorption capacity calculated using the DR equation (benzene, W_0 : 0.5 ml/g, E_0 : 17.185 KJ/mol, RT: 2.4486 KJ/mol), upper plot: relative pressure up to 30%; lower plot: lower relative pressure.

Background

It has been suggested that the affinity coefficients can be approximated by ratios of:

1) molar polarizabilities (α),

$$\beta = \frac{\alpha}{\alpha_{REF}} \quad (3-3)$$

2) molar volumes (V) of the adsorbates in the liquid state,

$$\beta = \frac{V}{V_{REF}} \quad (3-4)$$

3) ratios of parachors (Ω) of the adsorbate and a reference compound.

$$\beta = \frac{\Omega}{\Omega_{REF}} = \frac{\left[V\gamma^{\frac{1}{4}} \right]}{\left[V\gamma^{\frac{1}{4}} \right]_{REF}} \quad (3-5)$$

where γ = surface tension and V = molar volume of the adsorbate.

These three expressions have been compared by Wood (2001), who concluded that these three methods give comparatively good predictabilities, but that power functions with exponents less than unity provided slightly better fits for predicting experimental values. The author recommended the molar polarizability correlation parameter.

The predictive power of different models and the criteria for selecting reference compound(s) are, however, still under discussion (Reucroft et al. 1971, Noll et al. 1989, Golovoy and Braslaw 1981). Reucroft et al. and Noll et al. concluded that the vapors under consideration and the reference vapors should be of similar polarity, while Golovoy and Wood (Wood 2001) expressed the view that a single reference compound would be sufficient. The Eqs.(3-3) to (3-5) correlate β with one or two parameters of the adsorbate, but these equations sometimes produce very different results. To resolve these problems it is necessary to start with a systematic examination of the inherent nature of the affinity coefficient.

Background

3.3.2 Dynamic adsorption in activated carbon beds

Initially, when a contaminated gas stream passes through a packed carbon bed (see Fig. 3.5), most of the contaminant, the adsorbate, is adsorbed in the vicinity of the inlet to the bed. The gas then passes on with little further adsorption taking place. Later, when the inlet part of the adsorbent becomes saturated, adsorption takes place deeper inside the bed. As more gas passes through and adsorption proceeds, the so-called mass transfer zone (MTZ) moves forward until the breakthrough point is reached. If the flow of gas is continued, the exit concentration from the bed will rise gradually until it reaches the level of the inlet concentration. At this point, the bed is fully saturated. The simplest case, when the gas stream is challenged with one organic vapor, is illustrated in Fig.3.6. The service life of the filter bed is regarded as the time when the exit concentration has reached an unacceptable level.

When packed beds of activated carbon are used for removing gases and vapors from air streams, it is essential to know their efficiencies and service lives to facilitate application, design and maintenance decisions. Predictive models of service life should incorporate adsorbate properties, adsorbent properties, bed geometries and the conditions of use (Wood, 2002).



Fig.3.5: Diagram of a fixed bed of activated carbon particles.

Background

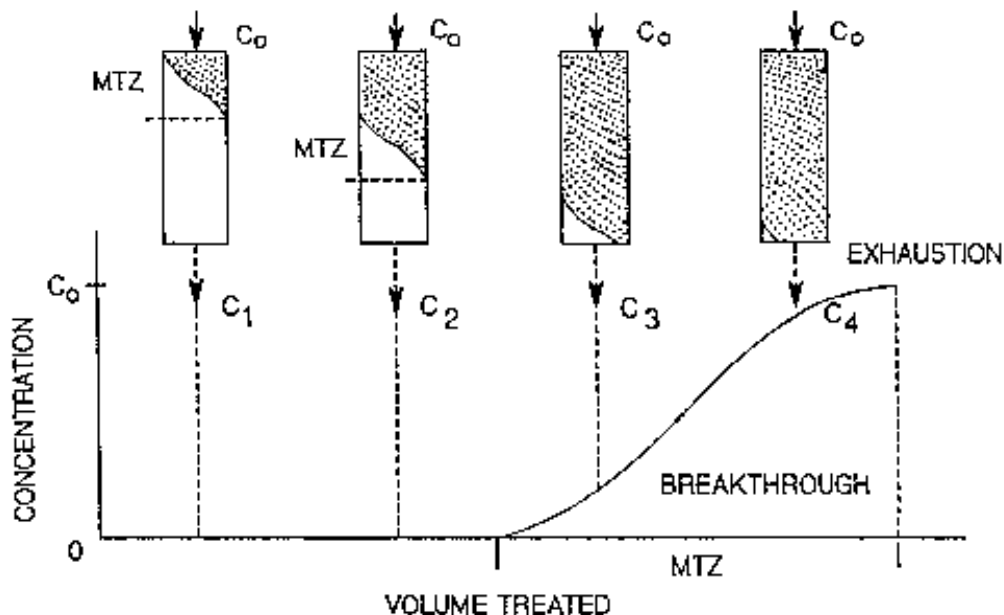


Fig. 3.6: Idealized breakthrough curve of a fixed bed adsorber.

Several models to predict the breakthrough curves for physisorption of organic vapors have been proposed: Mecklenburg's expression (Klotz, 1946); the modified Wheeler equation (Wheeler and Robell, 1969; Jonas and Rehrmann, 1974); the Wheeler-Jonas equation (Vermulen et al., 1984; Lodewyckx and Vasant, 1999), also known as the 'ideal' reaction kinetic equation (Wood and Stampfer, 1993); and the Yoon-Nelson equation (Yoon and Nelson, 1984). All these equations are based on a mass balance assuming that the quantity of vapor entering the bed equals the mass of vapor adsorbed plus the mass of vapor penetrating the bed. The similarities between these models have been analyzed by Yoon and Nelson (1984).

Among these, the Wheeler-Jonas equation is the most widely used to estimate the breakthrough time of organic compounds on activated carbon (NIOSH, 1977). It has a simple form, with some parameters readily available from the literature or from carbon manufacturers, and it is known to yield good predictions for breakthrough times (Wood and Moyer, 1989). It has recently been shown that the Wheeler-Jonas equation has a wider scope of application than just physisorption for a constant flow pattern (Nir et al., 2002; Lodewyckx et al., 2003).

Background

The Wheeler-Jonas equation takes the form:

$$t_b = \frac{W_e W}{C_0 Q} - \frac{W_e \rho_B}{k_v C_0} \ln \left[\frac{(C_0 - C_x)}{C_x} \right] \quad (3-6)$$

where

t_b = time to reach the breakthrough fraction $b = C_x/C_0$ (min)

C_0 = bed inlet concentration (g/cm³)

C_x = chosen breakthrough concentration (g/cm³)

W = weight of the carbon bed (g_{carbon})

W_e = equilibrium adsorption capacity of the carbon for a given vapor (g/g_{carbon})

Q = volumetric flow rate (cm³/min)

ρ_B = bulk density of the carbon bed (g_{carbon}/cm³)

k_v = overall adsorption rate coefficient (min⁻¹)

To use this equation, two parameters, W_e and k_v , must be determined. This can be done either experimentally or by extrapolation from measurements using a reference adsorbate. The first parameter W_e , the adsorption capacity, is usually calculated from an adsorption isotherm equation (Wood and Moyer, 1991); the Dubinin-Radushkevich equation is often used in the case of organic vapor adsorption. It should, however, be remembered that a slight deviation between the calculated equilibrium adsorption capacity and the effective adsorption capacity required for Eq. (3-6) may introduce a significant error into the estimated breakthrough time. This is demonstrated in Fig. 3.7a. The figure shows the effect of a small error of 5% in W_e . The effect is almost constant over the concentration range and more severe for benzene than for acetonitrile. This is because benzene has a higher W_e than acetonitrile. In practical applications of Eq. (3-6) it is therefore advisable, as a safety precaution, to reduce the value of W_e calculated by the DR-equation by 10% in order to avoid overestimation of the breakthrough time.

Background

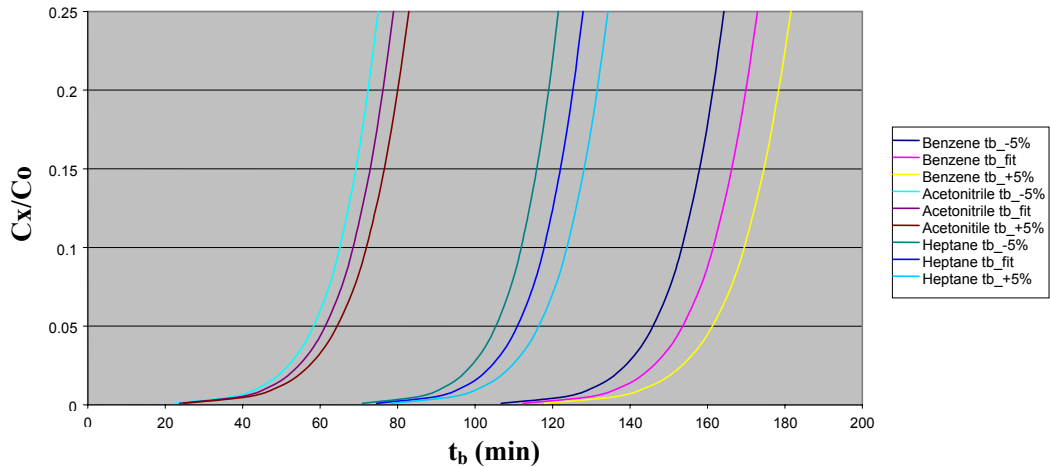


Fig. 3.7a: The effect of a 5% error in W_e when calculating breakthrough time.

The second term, k_v , the overall adsorption rate coefficient, represents the influence of the adsorption dynamics on the breakthrough time. Fig. 3.7b which shows the effect of a 20% error in k_v demonstrates that the breakthrough time is less sensitive to an error in k_v than in W_e .

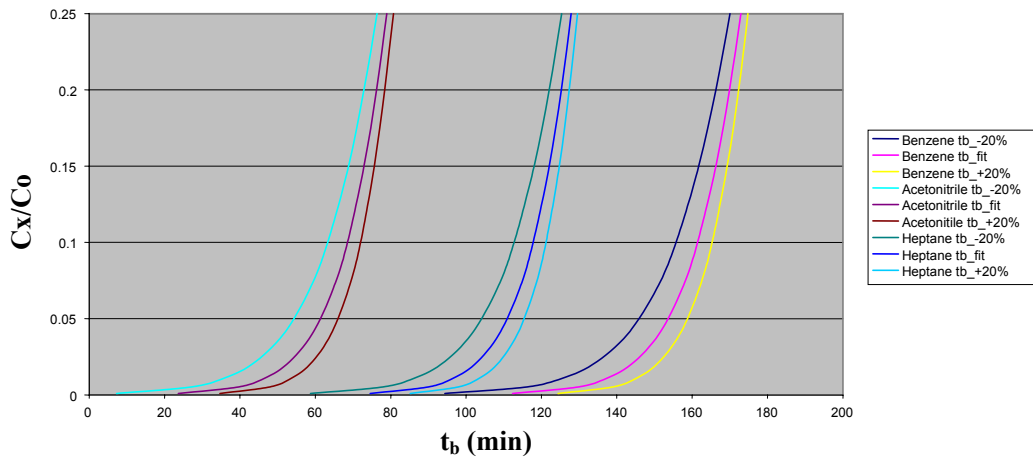


Fig. 3.7b: The effect of a 20% error in k_v when calculating the breakthrough time.

Background

The effect on breakthrough time is, however, more pronounced in the first part of the breakthrough curve (Fig. 3.7b). A good predictive model for k_v would, therefore, improve the prediction of breakthrough time, especially in the lower range, when using the W-J equation.

The rate coefficient k_v is somewhat difficult to predict. There are, however, some models available (Jonas and Svirbely, 1972; Jonas and Rehrman, 1974; Wood, 1993; Lodewyckx and Vasant 2000).

First, k_v cannot be measured directly experimentally; it has to be calculated either from the breakthrough time or from breakthrough curves. Therefore, it inevitably carries experimental uncertainties. Second, there are different philosophies regarding how k_v should be calculated from Eq. (3-6), as recently summarized in a review by Wood (2002). Even when the same approach is used to calculate k_v , for instance from a plot of $\ln[(C_0 - C_x)/C_0]$ vs. time t_b for varying C_x/C_0 ratios, the outcome will be different if there is a slight curvature in the line and different breakthrough ranges have been chosen. It is therefore highly desirable for the ways of calculating k_v to be examined and a standard method for its derivation to be developed. Model development and model comparison should be based on a standardized method for calculating k_v .

Three different methods for deriving k_v from Eq. (3-6) are available:

1. Breakthrough time t_b is plotted vs. varying bed weight at a fixed C_x/C_0 . k_v is obtained from the slope and intercept of the regression line.

Large errors will be introduced if the extrapolated intercept is close to zero. In addition, the calculated value of k_v is dependent on the breakthrough fraction chosen.

2. k_v is calculated for one specific breakthrough fraction from the difference between the breakthrough time and the stoichiometric point (t_{sto}) (Wood, 1993) or by using a known W_e value (Lodewyckx and Vasant, 2000).

The t_{sto} is often close to $t_{50\%}$. It has therefore been assumed that Eq. (3-6) is valid for describing the breakthrough curve up to approximately 50%. This approach, however, does not compensate for any random error in the observation data, because only two points define the line. This approach, therefore, attributes the experimental error in measuring breakthrough time to the variation in k_v for different breakthrough fractions. Small errors in t_{sto} and $t_{0.1\%}$ are propagated into large errors in k_v as the difference between the two becomes smaller (Wood and Lodewyckx, 2003). When Lodewyckx and Vasant found the repeatability of calculating k_v using a two-point method (0.1% and 1% breakthrough fractions) to be insufficient, they changed to an alternative method: by using a value of W_e predicted from the DR equation together with $t_{0.1\%}$, $k_{v0.1\%}$ can be calculated from Eq. (3-6).

Background

3. A plot of $\ln[(C_0 - C_\infty)/C_\infty]$ vs. time t_b for varying C_∞/C_0 . k_v is derived from the slope and intercept of the regression line.

This approach employs the least-squares method to calculate the line of best fit to multiple points on the breakthrough curve. The random error in the observations is taken into account as part of the regression calculations. However, the range of the breakthrough fractions is important for the derivation of the slope and intercept since the breakthrough curve is not perfectly symmetrical. The linear range must, therefore, be determined and the range of breakthrough fractions defined before modeling commences. This approach is the one used in this work to calculate k_v for the initial part of the breakthrough curves (Wood and Moyer, 1989).

3.3.3 Existing models for the adsorption rate coefficient

Three models for predicting k_v have been developed, based on values of k_v derived from the methods described above. A model proposed by Jonas et al. (1974) uses k_v derived according to method 1 at a 1% breakthrough fraction as follows:

$$k_v = 111.6 v_L^{1/2} d_p^{-3/2} \quad (3-7)$$

where v_L is the superficial linear velocity in cm/sec and d_p the granule diameter in cm.

If another breakthrough fraction had been used, Eq. (3-7) would have a different form. In addition, this model does not account for the influence of properties of the adsorbate.

An alternative model suggested by Wood is based on a large number of k_v values calculated from experimental breakthrough curves using method 2:

$$k_v = \left\{ \left[\left(\frac{1}{v_L} \right) + 0.027 \right] * \left[0.000825 + \frac{0.063 - 0.0058 \ln \left[\frac{(C_{in} - C_{out})}{C_{out}} \right]}{P_e} \right] \right\}^{-1} \quad (3-8)$$

where v_L = linear velocity (cm/sec)

P_e = molar polarization of the adsorbate (cm³/mol)

C_{in} = inlet concentration (ppm)

C_{out} = chosen exit concentration (ppm)

The influence of the properties of the adsorbate on the value of k_v is introduced through P_e in this equation. The dependence of the breakthrough fraction is accounted for in the model, but the influence of the adsorbent is not taken into account.

Background

Another equation has been suggested by Lodewyckx and Vasant:

$$k_v = \frac{C\beta^x v_L^y}{d_p^z} \quad (C = 48, x = 0.33, y = 0.75, z = 1.5) \quad (3-9)$$

This model is based on a k_v value calculated at the 0.1% breakthrough fraction using a known adsorption capacity, W_e . It is comparable to the two-point method used by Wood since W_e is related to the stoichiometric time. The model does not take into account the random experimental error introduced by using only one point on the breakthrough curve. The value of k_v calculated by Eq. (3-9) is, therefore, strictly valid only for breakthrough fractions close to 0.1%. Furthermore, the constants C , x , y and z in Eq. (3-9) were obtained by relating k_v to one specific variable (β , v_L or d_p) at a time while keeping the other two constant. This procedure, therefore, assumes that these factors vary independently of each other.

Wood and Lodewyckx (2003) developed a new model of k_v based on Eq. (3-8) and (3-9), in which the adsorption capacity was introduced as a variable to k_v too.

A feature missing from the majority of the models is that they are not based on a systematic investigation of the parameters that might influence k_v , such as velocity, inlet concentration, carbon properties and compound properties.

In this work, different approaches for calculating k_v from breakthrough data are examined and reviewed. A procedure for calculating k_v is proposed in which random experimental errors have less influence than in previous approaches. A new model is then developed using multivariate data analysis to study the relationship between k_v and the properties of the adsorbate, adsorbent, and the air velocity. The performance of the Wheeler-Jonas equation for predicting breakthrough time is refined by improving the accuracy of predicting k_v for organic compounds.

3.4 Multi-component adsorption

In most practical adsorption processes, there is more than one component to be adsorbed. Measurements of the adsorption capacities of multiple-component mixtures are much more complex than for a single adsorbate. The possibility of predicting multiple-component adsorption equilibria from pure component adsorption isotherms has been under investigation for many years in applied adsorption research. This would be useful because the adsorption capacities of each component in the vapor mixture are key parameters when estimating the service life of activated carbon beds.

Background

One approach to obtaining equilibrium capacities of mixtures is the ideal adsorbed solution theory (IAST), developed by Myers and Prausnitz (Myers and Prausnitz, 1965; Myers, 1968). Many other approaches have been proposed: vacancy solution theory (Suwanayuen and Danner, 1980); density functional theory has been applied to binary mixtures (Bhatia, 1998); statistical thermodynamics have been used (Bering et al. 1977; Jakubov et al., 1977; Nguyen and Do, 2001); and the Dubinin-Astakhov equation has been applied (Nieszporek K, 2002). However, IAST is the most widely used approach since it has several attractive features:

- (a) it requires no mixture data
- (b) it is an application of solution thermodynamics to the adsorption problem, and is thus independent of the actual model of physical adsorption (Ruthven et al. 1973; Ruthven, 1976; Myers, 2002).

The free choice of the isotherm equation leads to different applications of IAST (O'Brien and Myers 1985; Wood, 2002). For example, the so-called Myers-Prausnitz and Dubinin (MPD) method developed by Lavanchy and Stoeckli (Lavanchy et al. 1996; Lavanchy and Stoeckli, 1997) is the combination of IAST with Dubinin's theory of volume filling of micropores. Sundaram combined a modified DR isotherm with the IAST theory (Sundaram, 1995). The influence of the adsorption isotherm equation on predictions using IAST has been summarized by Richter et al. (1989).

The service life of a packed carbon bed challenged with binary adsorbates is often defined as the breakthrough time of the first-eluting compound. It could, however, be defined as the breakthrough time of the second-eluting compound if this compound is more toxic. Accordingly, the development of a theoretical model capable of predicting the service life of packed beds of activated carbon in the presence of a mixture of pollutants is very important. A system composed of only two compounds is the simplest type. It is, therefore, reasonable to start with theoretical studies of the adsorption behavior of binary adsorbate mixtures.

Compared with performance studies of packed carbon beds for a single adsorbate, only a limited number of investigations into the service life of binary systems have been reported (Jonas et al., 1983; Swarengen and Weaver, 1988; Cohen et al., 1991; Yoon et al., 1991 and 1992). Since the theories predicting breakthrough times for a single adsorbate are well developed, it would be useful if the relevant equations could be applied directly to binary systems. Some efforts have already been made to do this (Jonas et al. 1983; Wood, 2002). Jonas' approach was, however, based on only three binary mixtures, which were all combinations of carbon tetrachloride, chloroform and benzene, and changes in the adsorption rate coefficients of the compounds in the binary mixtures were not considered, although they deviate strongly from the values of the corresponding single compounds. Wood's approach to deriving the breakthrough time is incomplete because his investigation considered only the change in the adsorption rate coefficient and not the

Background

adsorption capacity. Other authors have proposed theoretical or mathematical methods for predicting the complete breakthrough curves of binary or multiple adsorbates (Yoon et al., 1991 and 1992; Vahadat et al., 1994; Lavanchy and Stoeckli, 1997 and 1999). These methods have several drawbacks which reduce their general applicability:

- 1) some experimental data for the binary systems are needed (Vahadat et al., 1994);
- 2) the methods have been developed on the basis of only one or two specific binary organic mixtures, and may not be representative for other mixtures.

Since it is impractical to test for all possible combinations of organic compounds, information is needed on the way in which physico-chemical properties of vapors affect adsorption, and thus breakthrough time. Robbins and Breysse (1996) tried to correlate the properties of binary mixtures with their breakthrough times, but the properties were limited to compound polarity and boiling point.

When the constituent compounds have similar physical properties and form an ideal mixture in the liquid adsorbed phase, co-adsorption is the predominant mechanism during the early period of breakthrough. In this case, the W_e of both compounds in the binary systems could be predicted using IAST theory, as applied in the MPD approach developed by Lavanchy and Stoeckli (1997), provided that all input parameters are available.

A procedure for predicting adsorption equilibria of binary adsorbates using IAST in combination with the Freundlich equation was developed as part of the work underlying this thesis and the calculation was compiled into a computer program.

IAST is valid for mixtures of adsorbates composed of compounds with similar properties and hence forming an ideal solution in the adsorbed phase.

This thesis, therefore, presents a method for predicting the initial part of the breakthrough profile for both components of binary organic vapor mixtures based on an extension of the W-J equation. The method was developed using nine binary combinations of vapors, selected in such a way that they cover a diversity of physical properties. The present work focuses on binary mixtures of dissimilar compounds, where the IAST method is likely to fail.

4 MATERIALS AND METHODS

4.1 Statistical experimental design

Experimental designs, such as factorial design (FD) and fractional factorial design (FFD), provide a way to systematically and simultaneously alter a set of variables which are orthogonal to each other, thus ensuring that the whole experimental domain is covered (Box et al. 1978 and Eriksson et al. 2000). It is an efficient strategy for reducing the number of experiments when many factors have to be considered at the same time. When building a model for predicting the breakthrough time of organic compounds, physico-chemical properties of adsorbates, properties of the adsorbent and experimental conditions are all factors that need to be considered.

In order to study the influence that properties of organic compounds have on adsorption performance, a representative set of adsorbates is needed for experimental evaluation. Therefore, a subset of organic compounds was selected to cover a sufficient range of variation in properties. Experimental design based on independent variables extracted from compound properties ensured that the selected organic compounds were representative.

FD and FFD are illustrated in the following figures, using a three factor, two-level design as an example.

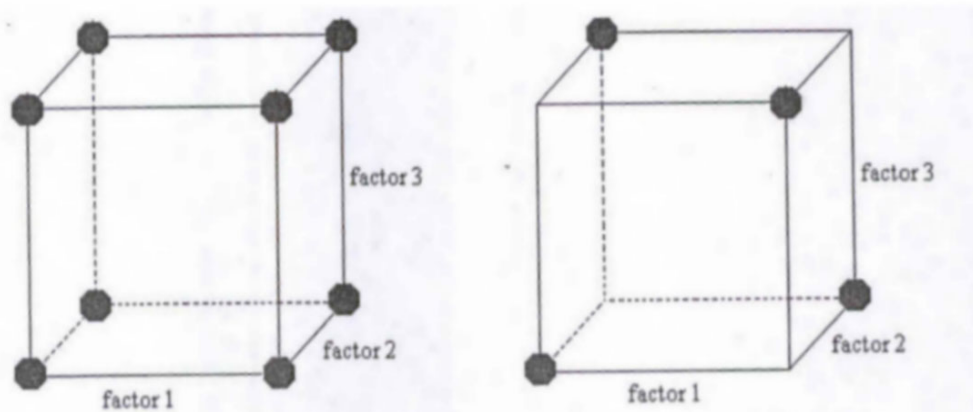


Fig. 4.1a: Factorial Design 2^3

Fig. 4.1b: Fractional Factorial Design 2^{3-1}

4.2 Selection of adsorbates

The adsorption process is complex. It is affected not only by parameters related to the physico-chemical properties of the adsorbate and adsorbent but also by environmental conditions. The range and variety of volatile organic contaminants present in industrial and other work-place environments is large, and thus they have diverse physico-chemical properties. For practical reasons, it is impossible to run experiments using all relevant compounds to acquire information about the relationship between their properties and the resulting adsorption capacities and breakthrough times. The strategy proposed in this thesis is to select a representative subset of VOCs to use in the development of predictive models. The subset selected needs to cover all important dimensions of the physico-chemical property space.

4.2.1 Property descriptors of compounds

In this study, 68 common organic chemicals including hydrocarbons, halogenated hydrocarbons, amines, carbonyl compounds, alcohols, ethers and a few other compound classes were considered (Appendix I). As many as 45 parameters describing the physico-chemical properties of these compounds were either collected from handbooks (Riddick et al., 1986; Lide, 1995; Howard et al., 1997) or calculated from their molecular structure (Sjöberg). To ensure an unbiased investigation of the compound properties that influence the adsorption mechanism, adsorption capacity and rate, it is important to consider as many property descriptors as possible. After an initial screening phase during model development, the most important descriptors were carried forward to the final model development stage.

Many of the macroscopic descriptors used for modeling are manifestations of the intrinsic properties of molecules that govern how they interact with their surroundings (Fängmark et al., 2002). Descriptors such as boiling point, melting point and vapor pressure reflect intermolecular forces. Variables that describe size include molecular weight, molar volume and van der Waals volume. Polarity is reflected by variables such as dipole moment, water solubility and Henry's law constant. Electronic polarizability is described by refractive index, dielectric constant, energies of frontier orbitals (HOMO and LUMO), and others. A summary of the descriptors is presented in Table 1, Paper I.

4.2.2 Principal component analysis (PCA)

The complete set of the 45 physico-chemical descriptors of organic compounds is too large to be used directly in the selection of representative compounds. Furthermore, some descriptors are correlated, and statistical experimental design requires independent factors.

Materials and methods

An efficient way to reduce the number of descriptors into a few independent variables is through the use of principal component analysis (PCA) (Wold et al., 1984).

PCA is an analytical projection method designed to extract the systematic variation in large data sets, to provide an overview of patterns and trends in the data. PCA calculates linear combinations of the original variables to produce a few independent dimensions or principal components (PC) that summarize the dominant variation in the data matrix. Imagine a swarm of points in multidimensional space, representing the physico-chemical properties of a number of relevant VOCs. By analyzing the latent structure in this data, it is possible to select a limited number of compounds that represent the whole set. PCA provides a simplification of the data matrix (X) as the product of two smaller matrices (T and P), comprising object scores and variable loadings, respectively, plus a residual matrix E . The data matrix X consists of N rows and K columns. Each row represents an object or observation (the compound in this case) and the columns contain the properties of each compound. Fig. 4.2 provides a schematic explanation of PCA.

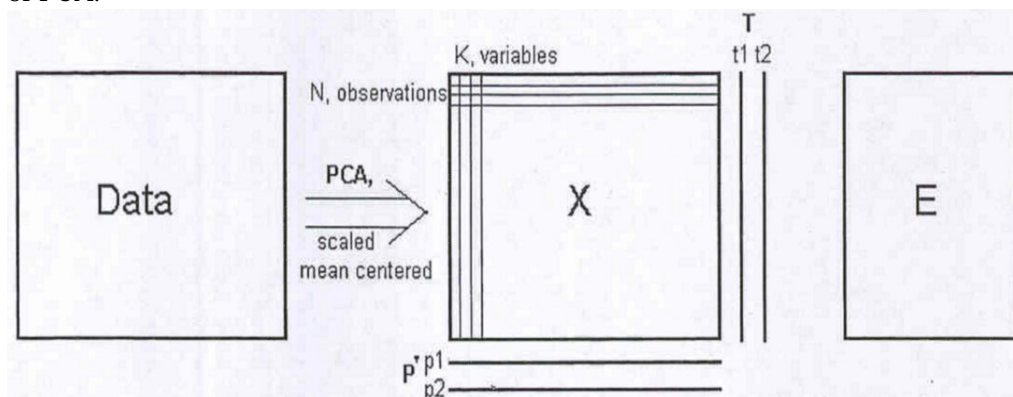


Fig. 4.2: Schematic explanation of PCA (courtesy of Umetrics).

Before analyzing the data, the original variables were mean-centered and scaled to unit variance. A line passing through the origin was fitted to the point swarm by means of the least squares method. This vector in the K -dimensional space is called the first principal component (PC1) and represents the direction of the greatest variation in the data. The second PC (PC2) is extracted from the residual information so that it reflects the second greatest source of variation in the data, and is orthogonal to the first PC. The size of the new matrices, T and P , depends on the number of PCs. When two PCs have been derived, they together define a plane: a window into the K -dimensional variable space, see Fig. 4.3. By projecting

Materials and methods

all the objects down onto this fewer-dimensioned sub-space and plotting the results, it is possible to visualize the structure of the data under investigation. The coordinate values of the objects on this plane are called scores (t_1 and t_2), and hence the plot of such a plane is known as a score plot. The PC score values can be considered as a new set of independent variables that describe most of the variation in the original data. The score plot depicts how the objects are related to each other.

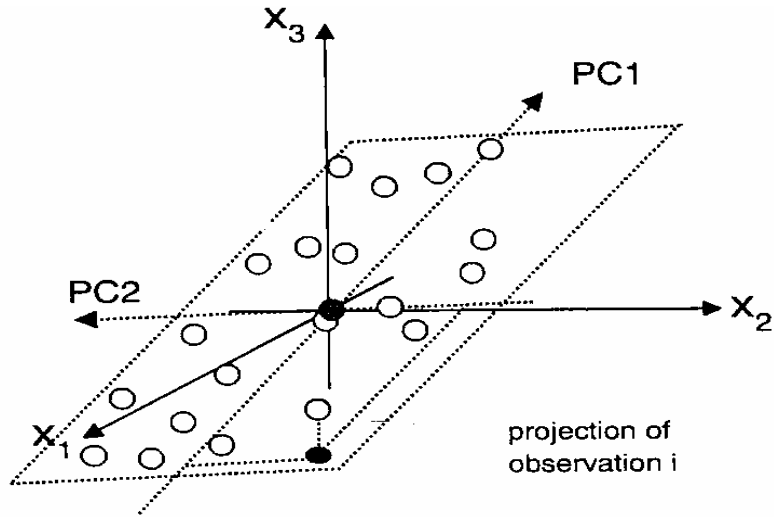


Fig. 4.3: The first PC, explaining most of the variation in a three dimensional space. The second PC is placed orthogonally to the first, and accounts for the second most variation in the point swarm. The two PCs form a plane. This plane is a window into the multidimensional space, which can be represented graphically (courtesy of Umetrics).

The orientation of this plane with respect to the original X variable axes defines the loadings (P). The loadings are calculated as the cosine of the angles between each of the old variable axes and each of the PCs. The P vectors are plotted against each other to show the impact of the original variables on the PCs. This plot is called a loading plot. A detailed description of PCA is given by Wold et al. (1984).

4.2.3 Selection of the training set as single adsorbates

The strategy for selecting single-component adsorbates was based on principal component analysis (PCA) and fractional factorial design. To illustrate the application of this strategy, reference is made to Papers I and II, where the original data matrix X with

Materials and methods

68 objects and 45 variables was reduced, using PCA, to a sub-space of five PCs. These five PCs account for 78.8% of the total variation in the data. The position of each compound within this space is defined by its score values. The score plot of the first two PCs is shown in Fig. 4.4. Since the derived PCs are orthogonal and consequently independent, they can be used as factors in a fractional factorial design to select a representative set of compounds. A 2^{5-2} design was adopted to suggest eight VOCs, forming a training set to be used for experimental evaluation and subsequent modeling. The compounds selected were benzene, acetonitrile, heptane, isopropylamine, 2-chloro-2-methylpropane, 1-chloropentane, dichloromethane and 2-butanone. In Paper IV four additional VOCs were considered. Their selection was based on the same principal components (PC) as described in Papers I and II, but using a different fractional factorial design (2^{3-1}). These compounds were propionaldehyde, 2-propanol, 2,2,4-trimethylpentane and 1,1,1-trichloroethane.

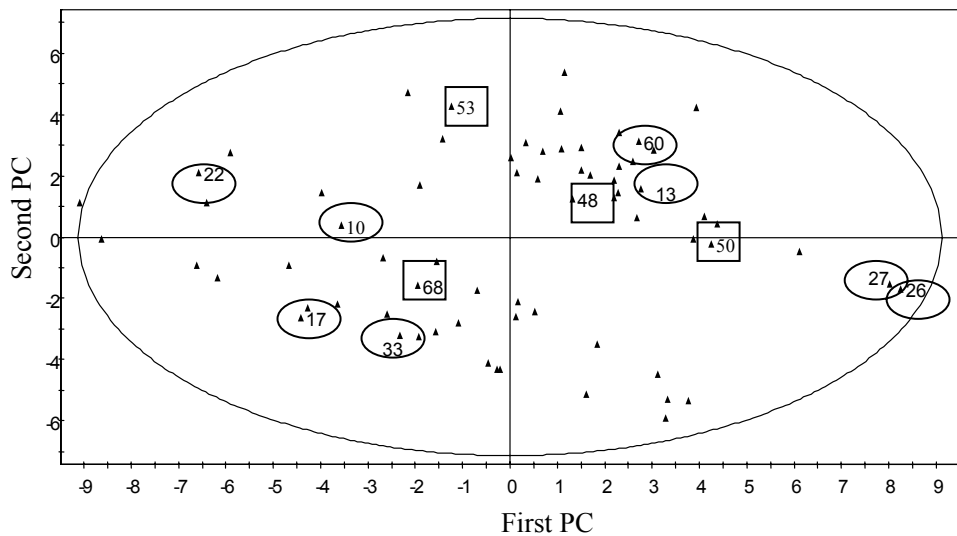


Fig. 4.4: The score plot of the first two PCs from the PCA of 68 compounds. The eight compounds selected as the training set used in Paper IV are marked with ellipses and the four compounds in the validation set are marked with squares.

Materials and methods

4.2.4 Selection of binary adsorbate systems

Randomly combining pairs of the eight compounds in Fig. 4.4 would produce 28 binary systems. It would be cumbersome and time consuming to study all these systems. It was decided, therefore, to select those compounds which had the largest differences in properties, since the aim was to study the influence of compound properties on breakthrough behavior. The selection was made by constructing a distance matrix based on the score values (t) of the five PCs. The elements in the distance matrix were calculated as follows:

$$S = \sqrt{\sum_i^5 [(t_{i1} - t_{i2}) R_i^2]^2} \quad (4-1)$$

where R_i^2 is the variance percentage of each score.

Pairs of compounds were selected for the binary systems that had maximal distances between them in the property space and do not react with each other. The distance matrix used in Paper V is shown in Table 1. Eight binary systems were selected: acetonitrile (1)—2-chloro-2-methylpropane (2) (22-48), acetonitrile—heptane (22-27), acetonitrile—1-chloropentane (22-50), acetonitrile—benzene (22-13), 2-butanone—1-chloropentane (68-50), dichloromethane—1-chloropentane (53-50), dichloromethane—heptane (53-27) and isopropylamine—heptane (33-27).

Table 1: distance matrix

Comp.(No.)	33	27	53	48	68	50	22	13
33	-							
27	6.52	-						
53	3.78	6.38	-					
48	3.30	4.41	2.32	-				
68	2.13	6.37	3.11	2.67	-			
50	4.71	2.73	4.14	2.17	3.92	-		
22	4.17	9.18	3.70	4.92	3.44	6.72	-	
13	4.20	4.36	2.84	2.11	3.34	2.11	5.77	-

In addition, three binary systems of compounds with quite similar properties were selected for comparison. These were: dichloromethane—2-chloro-2-methylpropane (53-48), benzene—1-chloropentane (13-50) and 2-chloro-2-methylpropane—benzene (48-13).

Materials and methods

4.3 The activated carbons used in this study

Three types of activated carbon were used as adsorbents in this study: peat-derived Norit R1 (Norit, The Netherlands) and coconut-derived AR1 and AR2 (Sutcliffe, U.K.). These three materials are commercially available and widely used for the adsorption of organic vapors (Linders 1999; Lodewyckx and Vasant 2000). The properties of the carbon sources used in this study are summarized in Table 2.

Table 2: Properties of the activated carbons used in this study

Carbon Type	R1 Extra	AR1	AR2
Form	extrudate	granule	granule
size	1 mm	12*20	8*16
Particle size (cm) 30%	0.108	0.147	0.186
Particle size (cm) 50%	0.099	0.132	0.169
Particle size (cm) 70%	0.093	0.118	0.157
Apparent Density ^a (g/ml)	0.703	0.731	0.775
Micropore Volume ^c (cm ³)	0.502	0.625	0.656
Mesopore Volume ^c (cm ³)	0.067	0.021	0.031
Packing Density ^b (g/ml)	0.449	0.393	0.426

^a: Measured using a Carlo Erba Macropores Unit 1120.

^b: Averaged from all the experimental runs.

^c: From the nitrogen adsorption isotherm.

The activated carbons were pretreated by heating them in an oven at 120°C for 18 hours, in order to remove any moisture.

As can be seen in Table 2, the three carbons are very similar with only slight variations in their physical properties.

Three other types of activated carbon were used in the work described in Paper III: fragmented coconut-derived activated carbon GH-28; pitch-based spherical activated carbon (J-1); and cylindrical activated carbon ZZ-07 from coal.

4.4 Experimental methods

4.4.1 Adsorption equilibrium measurements

The Headspace-Gas Chromatography technique was employed to determine adsorption isotherms. This is a relatively simple, rapid and accurate method for quantifying gas phase composition, and is, therefore, very useful in both research and routine work (Lavanchy et al, 1996; Linders et al., 1997)

Materials and methods

Fig. 4.5 shows a schematic representation of the procedure. A weighed quantity of adsorbent was introduced into a vial of known volume. The vial was sealed with a gas-tight Teflon-coated septum. In order to prevent the liquid adsorbate from coming into direct contact with the adsorbent, defined amounts of liquid organic compound were injected through the septum into a small vial residing inside the larger vial. After reaching equilibrium, the gas phase concentration of the adsorptive was analyzed by gas chromatography using a mass spectrometer as the detector. The amount adsorbed onto the activated carbon was calculated from the mass balance. By injecting varying amounts of the adsorptive, corresponding to different relative pressures of the compound in the vapor phase, adsorption isotherms were produced.

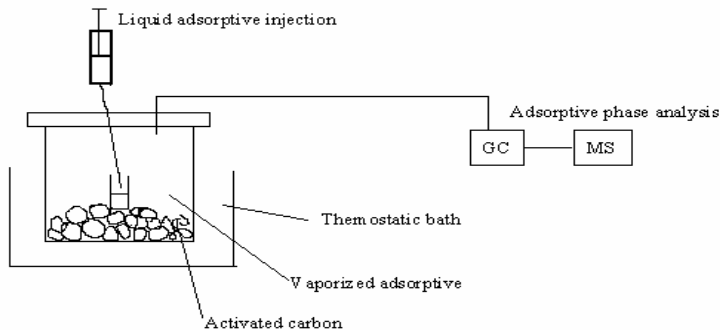


Fig. 4.5: Schematic representation of the Headspace GC technique.

Adsorption isotherms for eight VOCs, covering a relative pressure range from 10^{-6} to 0.4 (Sing et al., 1985; Chiang et al., 2001), were measured. A more detailed description of the experimental procedure is presented in Paper I.

In the studies described in Paper III the same experimental procedure was used for binary systems, except that the two chemicals were injected consecutively into the vial.

4.4.2 Breakthrough measurements

Fig. 4.6 is a schematic representation of the experimental set up for measuring the breakthrough curves of organic compounds on fixed-activated carbon beds. Purified and dried compressed air at room temperature (20 ± 1 °C), regulated by a mass flow controller (Bronkhorst, The Netherlands), was challenged with each organic vapor. The amount of challenge vapor was regulated by a liquid mass flow meter (Bronkhorst, The Netherlands). To determine the breakthrough curves of binary adsorbates, two liquid mass flow meters

Materials and methods

were used to regulate the respective flow rates of the liquids. The air-VOC mixtures were homogenized in a static mixer and directed towards the adsorbent. The adsorbent holder was a steel cylinder, 3.2 cm in diameter and 3.0 cm in depth. The flow rate of the compressed air, the injection flow rate of the challenge compound and the temperatures of the vapor generation equipment and mixer were computer-controlled.

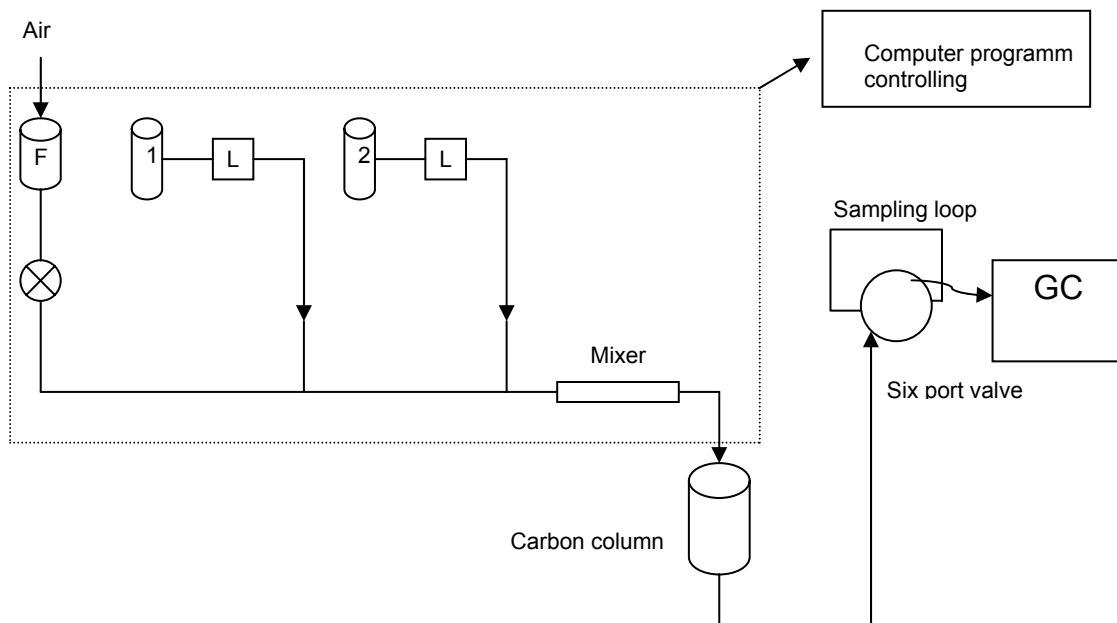


Fig. 4.6. Schematic representation of the breakthrough experimental set-up.

Steady-state flow velocities were set to 11.32 cm/sec (5.46 l/min) and 16.98 cm/sec (8.19 l/min). These volumetric flow rates, scaled up to the dimension of a common protective mask cartridge (10 cm in diameter), correspond to breathing rates of 53.3 l/min and 80 l/min. These rates are representative of flows at a moderately heavy work load and a somewhat heavier work load, respectively (Yoon and Nelson, 1984; Vahdat et al, 1994). A limited number of experiments were also performed at 14.14 cm/sec, i.e. the mean flow rate.

Materials and methods

The inlet concentration was set to 1000 ppm in all cases, since preliminary experimental results, and previous work (Jonas and Svibely, 1972; Wood, 1992), indicated that inlet concentration has a negligible influence on k_{p} .

The inlet and outlet concentrations of the challenge vapor were analyzed using a gas chromatograph (AutoSystem XL-GC, Perkin Elmer Inc., USA.) fitted with an automatic sampling loop (100 μl), a HP-5 capillary column and a flame ionization detector. The outlet concentration, sampled every 5 to 10 minutes, was recorded up to 100% breakthrough. At a minimum, duplicate experiments were performed for each combination of experimental conditions.

4.5 Modeling

4.5.1 Partial least squares projection to latent structures (PLS).

PLS is a multivariate projection method closely related to PCA. The aim of PLS is to find a relationship between a factor matrix (X) and a corresponding response matrix (Y). PLS is a powerful tool for analyzing data with many, noisy, collinear, and even incomplete variables. In a manner similar to PCA it extracts the latent structure of both X and Y data matrices and establishes a correlation between the two. The new projected latent variables or vectors are calculated such that the first vector describes the highest correlation between X and Y, the second vector the second highest correlation and so on. The vector is a straight line, fitted to the observations, through the average of each point swarm. By projecting the points (observations) onto this vector, the so-called score values are obtained. The score values of all observations form the first X-score vector, t_1 . The same procedure is applied to the Y matrix, where the highest correlation is described by the first Y score vector, u_1 . Vectors t_2 and u_2 can then be calculated in the same way from the residual information. The vectors t_1 and u_1 are related to each other by the inner correlation: $u_1 = t_1 + h_1$, where h_1 is the residual. Predictions can then be made by inserting the x-variables from an observation into the model and using the inner relationship between t and u to predict the unknown y (see Fig. 4.7).

Materials and methods

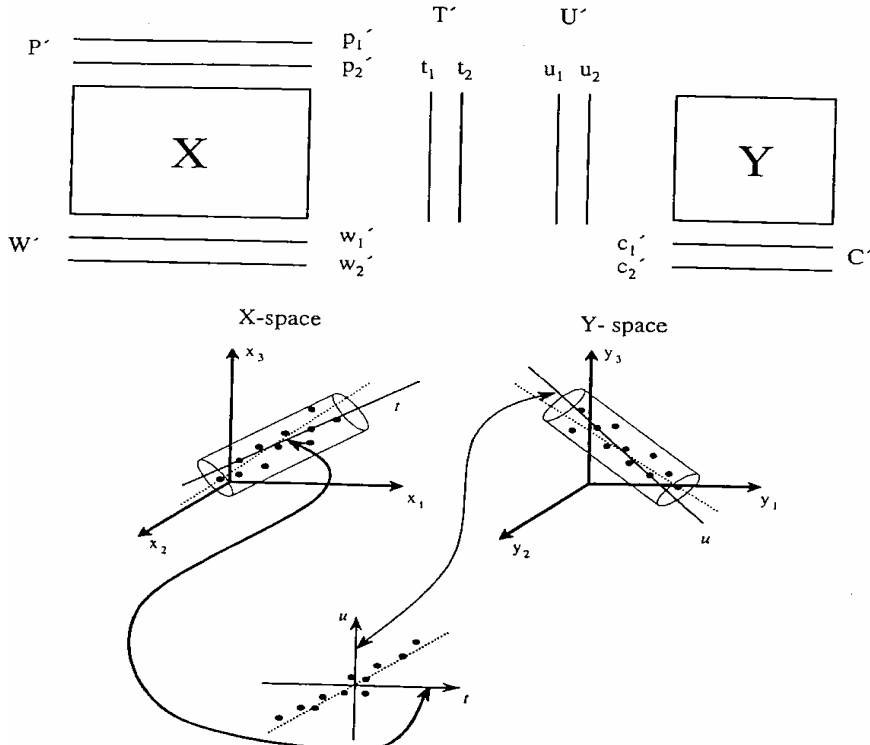


Fig. 4.7: Schematic explanation of the PLS method (Courtesy of Umetrics).

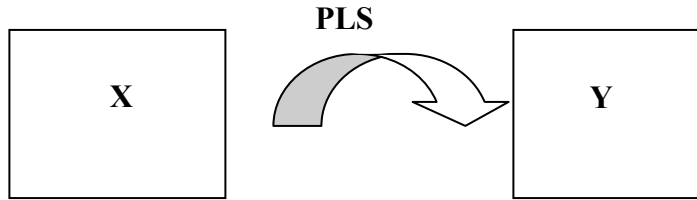
The PLS coefficients, B , are solutions to the equation

$$Y = XB \quad (4-2)$$

The regression coefficients can be expressed as:

$$y_m = b_0 + b_1 x_1 + b_2 x_2 + \dots + b_k x_k \quad (4-3)$$

The X- and Y-matrices that appear in Papers I, II, IV and V are summarized below.



Property descriptors:

Properties of selected adsorbate

Properties of selected adsorbate

Properties of adsorbate, adsorbent, velocity

Properties of selected binary adsorbates

Responses:

β (Paper I)

W_e (Paper II)

k_v (Paper IV)

R_{we1} , R_{kv1} , R_{we2} , R_{kv2}

(Paper V)

R_{we1} , R_{kv1} , R_{we2} , R_{kv2} are the ratios between the values W_{e1} , k_{v1} , W_{e2} , k_{v2} of the compounds in the binary mixture and the compounds as single adsorbates.

4.5.2 Model assessment and validation

The quantitative structure-affinity relationship (QSAfR) model is evaluated by simultaneously looking at the variance-explained R^2 (goodness of fit) and the variance of prediction Q^2 (goodness of prediction). The amount of variance described can be calculated for both the X and the Y matrices, resulting in the parameters R^2X and R^2Y . These two parameters are calculated according to the following formulae:

$$R^2X = 1 - RSS/SSX$$

$$R^2Y = 1 - RSS/SSY$$

where SSX represents the total variation in the X matrix, SSY represents the total variation in the Y matrix and RSS is the residual sum of squares.

The predictive capacity of the model (Q^2) is generated by cross validation (CV). In CV, the aim is to use only part of the data for model development, then to use the model to predict values for the unused data and compare them with the observed values. The squared differences between predicted and observed values form the predictive residue sum of squares (PRESS), giving the Q^2 value.

$$Q^2 = 1 - \text{PRESS}/SSY$$

R^2 and Q^2 are in the range 0 to 1. Usually, the larger the value of R^2 the greater the variation in the data that is explained by the PCs. The closer the value of Q^2 to 1, the better the model's predictive power. In general, $Q^2 > 0.5$ can be regarded as good and Q^2

Materials and methods

>0.9, excellent. Ideally, the difference between R^2 and Q^2 should be small, preferably not more than 0.2-0.3.

However, the only way to be absolutely sure of the predictive power of a model is to produce predictions for an independent external set of objects (a validation set), consisting of compounds not used in model development (Eriksson et al., 1993 and 1999; Wold, 1991). A comparison between the predictions and responses of the validation set will indicate the predictive power of the model.

In Paper I the validation set for prediction of β was composed of 40 compounds which were not included in the training set. Data for the 40 compounds were collected from the literature (Urano et al. 1982; Wood 1992 and 2001; Reucroft et al. 1971).

In Paper IV, four of the eight selected VOCs from Papers I and II were used as the validation set for the model of k_r .

5 RESULTS AND DISCUSSION

5.1 Modeling the affinity coefficient (Paper I)

Affinity coefficients, β , measured for the training set were subsequently correlated with experimental and calculated compound properties to develop a QSAfR model using PLS. The model was initially based on 45 physico-chemical properties of the adsorptive. Removing variables that did not significantly influence the prediction of β , and some variables correlated to them, resulted in a practical model based on three properties of the compound. These were: the calculated energy of the van der Waals interaction with a graphite model surface ($E_{\text{inter}}: \text{KJ/mol}$); the van der Waals volume ($Volume: \text{\AA}^3$); and the molecular weight ($M_w: \text{g/mol}$). The model takes the form:

$$\beta = -0.0731 + 0.0182 * M_w + 0.00418 * Volume - 0.0132 * E_{\text{inter}} \quad (5-1)$$

This model explains 98.9% of the variance in β , and the goodness of prediction, Q^2 , is 0.975. The internal validation criterion, Q^2 , is indicative of a very good model. This is also demonstrated by the improvement in prediction compared to the three traditional approaches for calculating β , see Fig. 5.1.

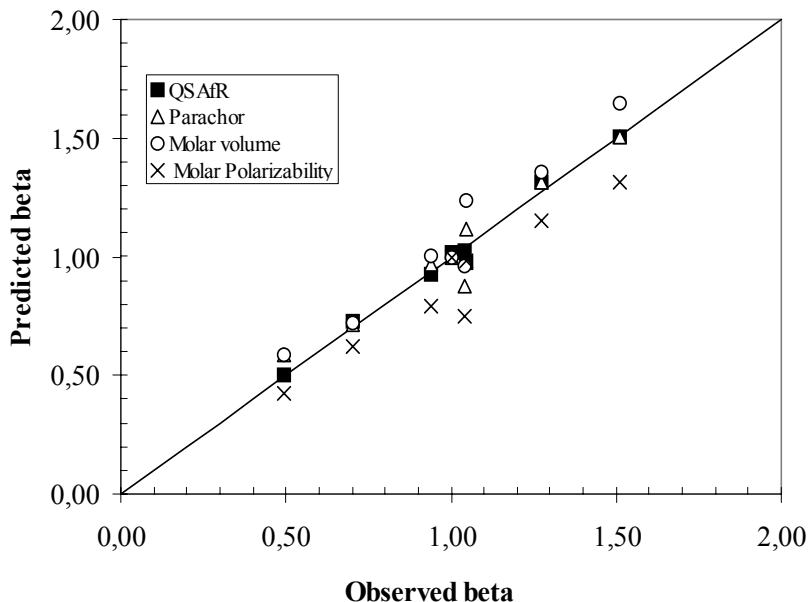


Fig.5.1: Comparison between observed and predicted values of β for the training set using the four different methods.

Results and discussion

To form an external validation set, experimental affinity coefficients of 40 other organic compounds (see Table 6 in Paper I) were extracted from the literature, and relevant property parameters calculated. The predictive power of the new model proved to be better than that of the other three models. This was confirmed by calculations of the root mean square error of prediction (RMSEP) of these four models: the RMSEP of the new model is 0.090, while calculations based on parachor, molar polarizability and molar volume yield RMSEPs of 0.141, 0.141, and 0.180, respectively. Furthermore, the prediction using the new model of β for formic acid is better than those obtained using any of the other three methods.

The model developed in this work has a higher predicting power for calculating the affinity coefficient than traditional methods based on parachor, molar polarizability and molar volume. The higher accuracy in prediction is valid for a large range of structurally diverse organic compounds. It demonstrates the importance of adding a descriptor for specific interactions with the carbon surface to size and shape descriptors.

5.2 The influence of compound properties on adsorption capacity (Paper II)

Paper II describes an investigation of the properties of the adsorptive that influence molar adsorption capacity during the early stages of adsorption. The paper describes the development of a quantitative structure-affinity relationship model that directly relates the adsorption capacities of a specific carbon to the properties of selected volatile organic compounds.

The molar adsorption capacities at five relative pressures (0.001, 0.01, 0.05, 0.1 and 0.15) comprised the matrix of responses and 45 variables describing the physico-chemical properties of the VOCs formed the matrix of factors. The model could be reduced to 16 compound properties described by two principal components and had an excellent correlation ($R^2 = 0.877$) and a reasonably good predictive power, $Q^2 = 0.713$.

The PLS loading plot (Fig. 5.2), which represents the relationships between factors and their influence on the measured responses, shows the distribution of responses in property space.

Results and discussion

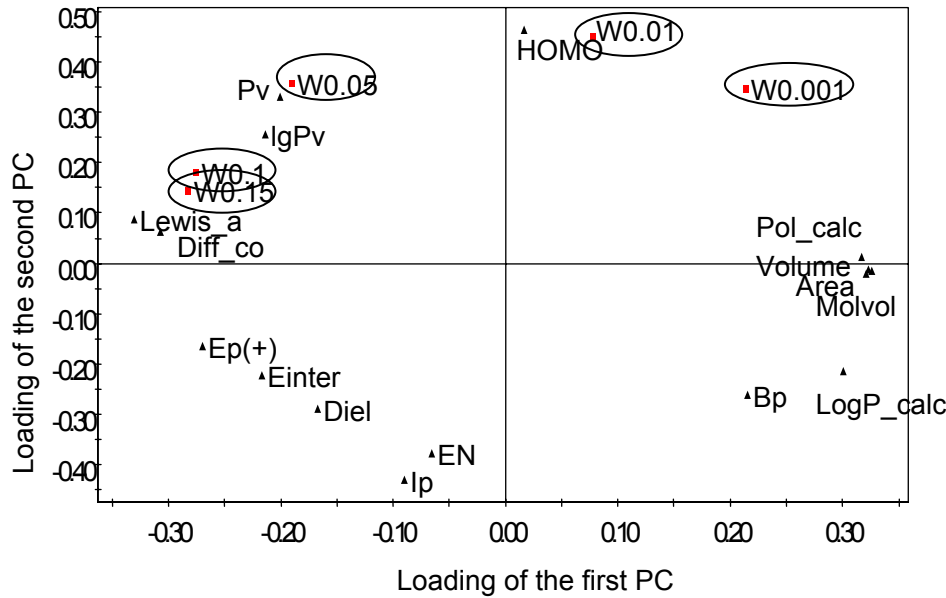


Fig.5.2: Loading plot of the QSAfR model based on all responses and 16 property descriptors.

As can be seen in the figure, at the lowest relative pressures, $W_{0.001}$ and $W_{0.01}$, the capacities are strongly influenced by the electronic properties of the adsorbate. These include the energy of the HOMO, ionization potential (Ip), and a parameter describing electronegativity (EN). The calculated energy of the van der Waals interaction with a graphite model surface (Einter) is also influential.

In contrast, at the highest relative pressures, $W_{0.1}$ and $W_{0.15}$, the molecular size (Volume and Area), the hydrophilic character of the adsorbate (logP), and other polarity descriptors (*Lewis_a*, *Ep(+)*, and *Diel*) have the greatest influence. In this pressure range, volatility parameters (*P_v*, *LgP_v* and *Bp*) also contribute.

The intermediate adsorption capacity, $W_{0.05}$, is affected by both groups of properties. Our modeling shows that the HOMO energy is an important factor in the early stages of adsorption. This is in agreement with previous observations on the adsorption of phenolic compounds on activated carbon (Furuya et al, 1997; Oskouie et al., 2002)

This work has demonstrated that the influence of the properties of the adsorbate varies according to the different stages of adsorption, reflecting the different mechanisms involved.

Results and discussion

5.3 Adsorption equilibria of binary systems (Paper III)

In this work, adsorption isotherms for pure benzene, n-hexane and n-pentane on the three types of activated carbon, at a temperature of 20 °C, were determined experimentally and fitted to the Freundlich and DR equations. It was found that the DR equation produces a better fit to the experimental data. However, because of the simpler mathematics, it was decided to use the Freundlich equation in combination with IAST. Fig. 5.3 shows that the phase diagram equilibrium line for benzene—hexane is quite close to the diagonal, but the lines for benzene—pentane and hexane—pentane are further away. This indicates that these two binary organic mixtures are easier to separate than the benzene—hexane mixture on the same activated carbon. This is a consequence of different adsorption affinities.



Fig 5.3: Adsorption phase diagram for the three binary systems on J-1 AC (at 20°C)

The experimental data were compared with the predicted values. It was found that the experimental results and the model predictions were in good agreement. The absolute mean deviation was lower than 10%, which is satisfactory. Deviations were observed at low values of composition and for tests using the J-1 activated carbon. There are probably

Results and discussion

two explanations for these deviations: the IAST model ignores interactions between adsorbates, and the Freundlich equation is used in IAST to predict the mixture adsorption (Richter, 1989). The Freundlich equation is unable to describe the adsorption isotherm of the pure component accurately at higher relative pressures. Further, the Freundlich equation does not equate to Henry's law at low coverage. The poor predictive power for the adsorbed phase composition on J-1 may also be due to the specific pore structure or heterogeneity of this pitch-based, spherical, activated carbon, and to the non-ideality of the adsorbed phase (Stoeckli et al, 2000).

5.4 Modeling the adsorption rate coefficient (Paper IV)

The three different approaches for deriving k_v from experimental breakthrough data, described in 3.3.2, were compared using the data for heptane on AR1 and AR2. The results are summarized in Table 1.

Table 1. Calculated k_v of heptane on AR1 and AR2 using different derivations.

	k_v (method 1)		k_v (method 2)		k_v (method 3)
	$t1\%$	$t10\%$	$t1\%$	$t10\%$	
AR1	12234	9665	3706	3101	4330
AR2	3634	10881	2553	2208	2846

method 1: Plot breakthrough time t_b vs. bed weight W_{AC} at fixed C/C_0 (1% and 10% respectively). k_v is obtained from the slope and intercept of the regression line.

method 2: One-point method with a known W_e value. W_e obtained gravimetrically from breakthrough experiments. The bed height is fixed at 3 cm.

method 3: Plot $\ln [(C_0 - C)/C]$ vs. time t_b for varying C/C_0 . k_v is derived from the slope and intercept of the regression line. The bed height is fixed at 3 cm. Breakthrough range 0~20%.

From Table 1 it can be seen that the three methods give different results and that the variation between the minimum and maximum value is large, between 400 and 500%. However, it is not possible from this comparison to determine which method produces the best estimate. For the reasons discussed in chapter 3.3.2 and because it covers the widest breakthrough range, method 3 was chosen.

A systematic investigation of the factors influencing k_v , including velocity and inlet concentration, was conducted using a two-level full factorial experimental design, Table 2.

Results and discussion

Table 2: Experimental design

Inlet concentration (ppm)	Velocity (cm/sec.)
1000 (-)	11.32 (-)
2000(+)	11.32(-)
1000(-)	16.98(+)
2000(+)	16.98(+)
1500(0)	14.14(0)

Experimental breakthrough data were collected for twelve compounds: benzene, acetonitrile, heptane, isopropylamine, 2-chloro-2-methylpropane, 1-chloropentane, dichloromethane, 2-butanone, propionaldehyde, 2-propanol, 2,2,4-trimethylpentane and 1,1,1-trichloroethane on Norit R1. Eight of the compounds were used as the training set to produce the model, and the remaining four compounds were used for validation.

Experimentally derived k_r values were modeled against velocity, inlet concentration and adsorbate properties using PLS. The modeling indicated that that inlet concentration had almost no influence on k_r and that velocity was the dominant factor. The initial full model was reduced by excluding descriptors that did not provide a significant contribution. Some correlated descriptors were also eliminated. The resulting model contains three significant PLS components that explain 91% of the variance in k_r . The loading plot of this model is shown in Fig. 5.4.

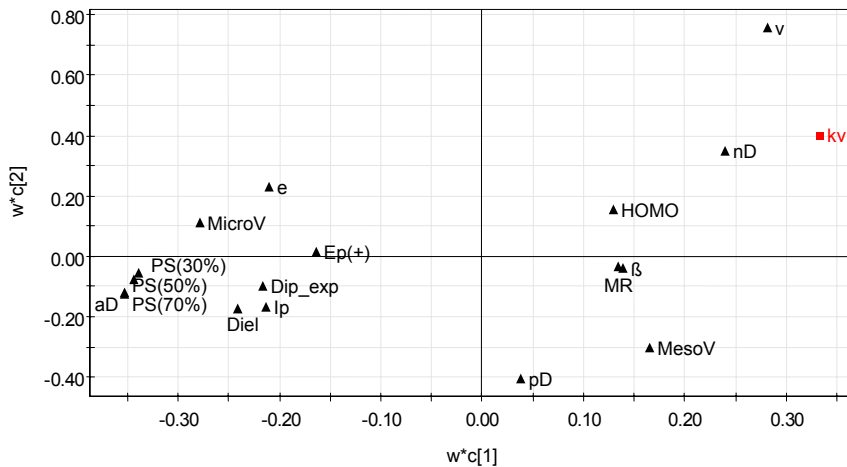


Figure 5.4: Loading plot for the first two principle components.

Results and discussion

Fig.5.4 shows that flow rate and carbon particle size, together with a few compound polarity descriptors, are key influences. A decrease in the ionization potential or an increase in the HOMO energy of the adsorbate seems to increase the rate constant. This is to be expected when molecular interactions at the carbon surface are involved in the rate determining step of adsorption.

A simpler and more user-friendly model, based on only three parameters, was then developed. The three parameters in the model are available from experimental conditions (flow rate), from handbooks on organic compounds (dielectric constant) and from sieve analysis of the carbon particle size. The model explains 87% of the variance in k_v and the value of Q^2 is 0.856. The prediction is satisfactory for both training and validation sets. Comparing different models for predicting k_v shows that the proposed model produces the best results. It should be noted, however, that the flow range investigated is limited to breathing rates found during the use of ordinary respirators. Further, the carbons investigated are designed to be used in respirator filters, making them rather similar in efficiency and particle size.

5.5 Prediction of the service life of carbon beds in the presence of binary adsorbates (Paper V)

In Paper V the results and data from research on the adsorption of single components are applied to the development of a method for predicting the initial part of the breakthrough profiles of binary organic vapor mixtures.

Breakthrough curves of eleven binary mixtures were measured on Norit R1 Extra. The curves are shown in Appendix III. It can be seen from the graphs that the first, less strongly adsorbed vapor, is displaced by the second vapor, giving the first vapor a higher maximum concentration than the input concentration. This is the so-called rollup phenomenon. Breakthrough times of both compounds decrease in comparison to their individual times.

The W-J equation is shown to be applicable to the breakthrough curves of both components of binary systems up to a 20% breakthrough ratio. This can be verified by checking the linearity of the plot of t versus $\ln((C_0 - C_x)/C_x)$. W_e and k_v can be calculated from the slope and intercept of the linear regression lines. It should, however, be stressed that the parameters W_e and k_v derived for binary mixtures cannot be interpreted in the same way as for single component systems. Despite this, they can be applied to predict the breakthrough curve up to the 20% breakthrough fraction.

The ratios of W_e and k_v for the components of the binary mixtures to the corresponding parameters for single component adsorption, R_{we1} , R_{kv1} , R_{we2} , R_{kv2} , were modeled using

Results and discussion

PLS. The modeling revealed that R_{ne1} and R_{kr2} depend on the properties of both compounds, while R_{kr1} and R_{kr2} can be considered to be constant.

Modeling showed that R_{ne1} was mainly influenced by the properties of compound 1, such as molecular size descriptors (van der Waals volume and area, molar volume), heat capacity, ionization potential, polarizability, the energy of van der Waals interaction with a graphite model surface and the affinity coefficient. It was also affected, to some extent, by the properties of compound 2, including the molecular size and dielectric constant.

R_{kr2} is influenced by the properties of both compounds: Lewis acid strength, polarizability, van der Waals volume, the affinity coefficient and energy of interaction with the graphite surface for compound 1, and Lewis acid strength, polarizability, heat capacity and energy of interaction with the graphite surface for compound 2.

Reducing the number of property descriptors, while taking into account their availability and importance for the performance of the model, resulted in a two-parameter model for R_{ne1} , explaining 87% of the variance ($Q^2 0.758$) and a three-parameter model for R_{kr2} explaining 90% of the variance ($Q^2 0.814$).

The property descriptors used for R_{ne1} are the molar volumes of the two compounds. For R_{kr2} the heat capacities of both compounds and the polarizability of the second eluting compound are used.

The breakthrough time of compound 1 in binary systems can be predicted by introducing the calculated W_{el} (binary) and k_{v1} (binary) values into the W-J equation. Calculated breakthrough times (t1% and t10%) of compound 1 for the nine binary systems are compared to the experimental values in Figs. 5.5 and 5.6. Calculations of the breakthrough times for compound 2, using 0.85 of R_{kr2} as recommended by Wood (2002), are also shown in the figures.

Results and discussion

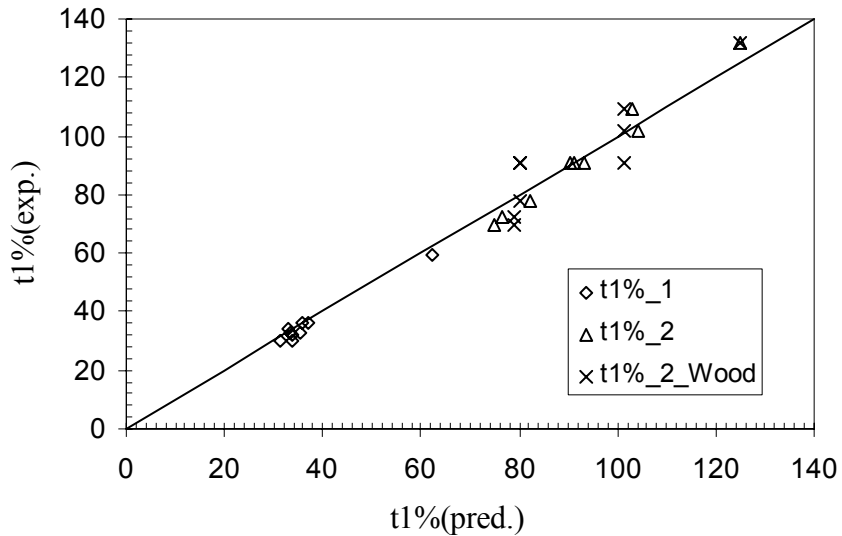


Fig.5.5: Prediction of breakthrough times at the 1% breakthrough fraction for both compounds of the nine binary mixtures.

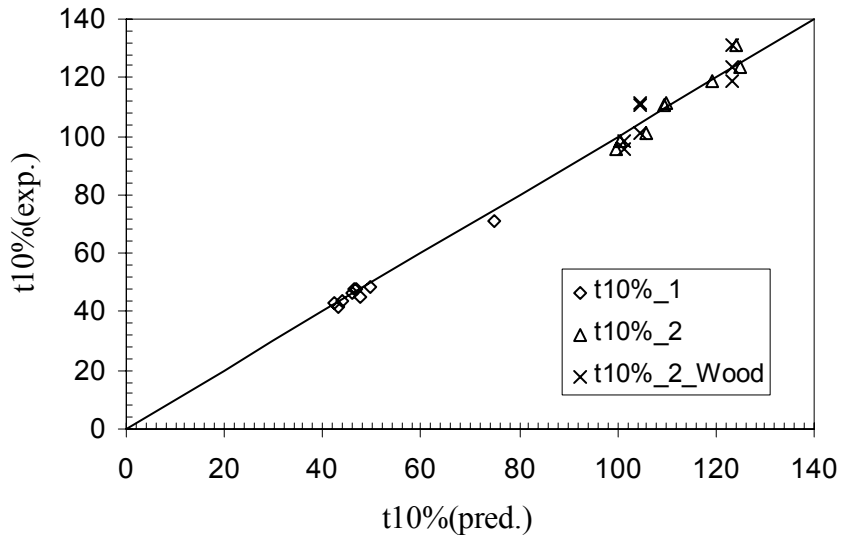


Fig.5.6: Prediction of breakthrough times at the 10% breakthrough fraction for both compounds of the nine binary mixtures.

Results and discussion

It is clear that the predicted breakthrough times for both compounds and both breakthrough ratios accord well with the experimental results.

We have shown that by modifying the Wheeler-Jonas parameters W_e and k_p the breakthrough curves of the compounds in a binary mixture can accurately predicted.

6 CONCLUSIONS

It has been demonstrated in this thesis that MVDA is a very useful technique to study the physisorption of organic compounds on activated carbons.

In order to draw conclusions of general validity, it is essential to select substances representing major regions of the physico-chemical property space. Therefore, a large set of structurally different compounds was reduced to a representative sub-set using PCA and experimental design. This sub-set was used in the experimental evaluation.

It was shown that adsorption parameters can be correlated to adsorbate properties, carbon properties and environmental conditions using PLS. The loading plot of the PLS analysis is an important tool for interpreting different aspects of adsorption.

PLS was also used in the development of predictive models for filter performance. The initial models containing a large number of variable descriptors could be simplified to user-friendly models with a few important and readily available parameters.

Traditional methods for calculating the affinity coefficient are based on parachor, molar polarizability and molar volume, all of which are mainly related to molecular size. This work demonstrates the importance of adding a descriptor related to specific interactions with the carbon surface.

It was found that HOMO energy is important for the adsorption capacity in the early stages of adsorption. This is consistent with findings related to liquid adsorption on activated carbon. During the later stages of adsorption, as super-micropores are filled, the adsorption capacity is governed mainly by molecular size.

It has been shown that breakthrough data for a wide range of compounds can be fitted to the Wheeler-Jonas equation up to at least a 20% breakthrough fraction with a correlation coefficient above 0.99. The merits of introducing a correction for skewness, as proposed by Wood and Lodewyckx are therefore debatable. The rate coefficient calculated using multiple points over a wide range of the breakthrough curve improves stability and accuracy.

PLS modelling of k_r showed that flow rate and carbon particle size, together with a few compound polarity descriptors, are important. Based on these findings a simple, user-friendly, three-parameter model was derived and validated. Comparing different models for prediction of k_r shows that the proposed model gives the best results. The model is limited to breathing rates valid for ordinary respirators and to common respirator filter carbons.

Conclusions

It was demonstrated that the W-J equation can be applied to the breakthrough curves of both components of binary systems for breakthrough ratios up to 20%.

The parameters characterizing the adsorption of each component in a binary system can be calculated from the corresponding single-component system data. Simple statistics showed that W_e of the second eluting compound and k_v of the first eluting compound can be considered to be constant.

Assisted by PLS modeling, a simple model for predicting W_e for the first eluting compound, based on the molar volumes of both components in the binary mixture, was developed. In a similar manner a model for k_v of the second eluting component was formulated. This model includes the heat capacities of both components and the polarizability of the second eluting compound.

The models proposed in this thesis have improved and simplified the prediction of filter performance for adsorption of single vapors and binary vapor mixtures. Thus, they should help improve the accuracy of estimations of filter service life.

7 FUTURE WORK

Although the strategy used in this work has given very promising results, there are a number of areas that need further investigation. These include:

- To extend the models for binary mixtures by including more compounds close to each other in property space.
- To check the validity of the proposed models at other challenge concentrations of the components of binary mixtures.
- To extend the flow velocity range to verify the limits of application of k_v .
- To investigate the influence of other carbon types and particle sizes.
- To include the effects of humidity.
- To investigate the possibility of modeling chemisorption.

Acknowledgements

8 ACKNOWLEDGEMENTS

First of all, I would like to express my sincere gratitude to my four supervisors: Professor Anders Cedergran for always doing his best to me and setting me up an example as a diligent scientist; Dr Ola Claesson, Dr Ingrid Fängmark, Lars-Gunnar Hammarström for their continuous scientific support and never ending encouragement in both academic world and everyday life. All of you have given me so much help that make me improve myself in profession area and feel at home in Umeå.

I want to say thanks to Lars Rittfeldt, Marianne Strömqvist, Per-Gunnar Jönsson from FOI for their valuable discussions and all help. Thousands of thanks to Stellan Brännström, Allan Abrahamsson, Melker Nordstrand for their help in the process of building the experimental set-up.

I also would like to show my gratitude to the whole Environmental and Protection Department in FOI for supplying me with a comfortable research and working environment. I would like to give my special thanks to Åsa Lundavall, who helped me edit this thesis and other reports and everything else. Sincere thanks to Åsa F, Åsa S, Birgitta, Christer, Christina E, Edvard, Erik, Göran, Hans-Göran, Håkan, Inga, Andreas, Jan(s), Jan-Olov, Jerker, Kenneth (tack för pimpling), Kristina, Lars Ö, Lennart, Leif, Martin, Pontus, Ronny, Rose-Marie, Sune(s), Tage, Thomas, Torbjörn, etc. for your friendliness and help. Thank the people working in library, in 'inköp', in the IT department, in NBC-analysis and Dan, Maine, Monica, Kurt etc. for help and support.

I would like to thank the whole Analytical Chemistry Department for their help when I had course and did assistant teaching work in the university. Thank you, Anita, Ann-Helen, Eric, Knut, Solomon, Michael, William, Johanna, Tom, Lars, Anna and all the others for your kind help.

Thousands of thanks to my friends in Umeå: Jin, Bo, Yu, Jiguang and Jinhan, Jian and Ming, Wen and Xiaolei, Xianzhi and Lin, Gangwei, Daoqun, Jiangbo, Hongjiang, Shujing and Yuqing in UK, André, Hasso and Peter; Annika, Karin, Martin, Thomas, Nettan and Eric from the nicest corridor I had been living in for two years, and Jon are all thanked for support. Thanks to my best friends: Camilla, Maria, Sandra and Linda. Thank you for helping me know more about your lovely country and warm accompany.

I also appreciate help and support from my former supervisors: Professor Kunmin Guo and Cunqiao Yuan, and colleagues: Hongyang Zhao, Lan Ma etc. in Beijing China.

Finally I want to say thank you Zijiu who was always there for me. I am grateful for all that you did for me. Parents, my lovely nephew: haohao, my sister and brother and all other families in China are thanked for love, care and support.

References

9 REFERENCES

Ackley MW. Residence time model for respirator sorbent beds. *Am Ind Hyg Assoc J* 46:679-89. 1985.

Aranovich GL, Donohue MD. Vapor adsorption on microporous adsorbents. *Carbon* 38:701-8. 2000.

Ashford RD. *Ashford's dictionary of Industrial Chemicals*. London: Wavelength Publishers, Ltd. 1994.

Baker FS, Miller CE, Repik AJ and Tolles ED. Activated carbon. *Kirk-Othmer Encyclopedia of Chemical Technology* 4: 1015-1037, 1992.

Battelle Memorial Institute. *The Development of a Fluidized Bed Technique for the Regeneration of Powdered Activated Carbon*. Washington: US Department of the Interior. 1970.

Bering BP, Serpinski VV, Jakubov TS. Osmotic theory of gas mixtures adsorption. 1. integral of Gibbs equation and adsorption isotherm. *Izv. Akad. Nauk SSSR. Ser. Khim.* 121-7. 1977.

Bhatia SK. Adsorption of binary hydrocarbon mixtures in carbon slit pores: a density functional theory study. *Langmuir* 14:6231-40. 1998.

Box GEP, Hunter WG and Hunter JS. Statistics for experimenters. Wiley, NY. Chichester, Brisbane, Toronto, 1978.

Brunauer S, Emmett PH and Teller E. *J Am Chem Soc* 60:309. 1938.

Cheremishinoff NP and Moretti AC. Carbon adsorption applications, in Cheremisinoff NP and F Ellerbusch (EDS.) *Carbon Adsorption Handbook*:1-53. Ann Arbor: Ann Arbor Science. 1978.

Chiang YC, Chiang PC, Huang CP. Effects of pore structure and temperature on VOC adsorption on activated carbon. *Carbon* 39:523-34. 2001.

Cohen HJ, Briggs DE and Garrison RP. Development of a field method for evaluating the service life of organic vapor cartridges—part III. Results of laboratory testing using binary organic vapor mixtures. *Am Ind Hyg Assoc J* 52:34-43. 1991.

References

Conner WC. In Physical Adsorption: Experiment, Theory and Applications (Fraissard J and Conner WC, editors). Kluwer, Dordrecht, p 33. 1997.

Dubinin MM., In Walker PL Jr., editor. *Chemistry and physics of carbon*, vol 2, New York: Marcel Dekker , 151-120. 1966.

Dubinin MM. Physical adsorption of gases and vapors in micropores. *Progress in surface and membrane science* 9:1-70. 1975.

Eriksson L, Jonsson J, Berglind R. External validation of a QSAR for the acute toxicity of halogenated aliphatic hydrocarbons. *Environmental Toxicology and Chemistry* 12:1185-91. 1993.

Eriksson L, Johansson E, Kettaneh-Wold N, Wold S. Introduction to Multi-and Megavariate Data Analysis using Projection Methods (PCA& PLS), Umetrics AB, p.490. 1999.

Eriksson L, Johansson E, Kettaneh-Wold N, Wikstrom C, Wold S. Design of Experiments: Principles and Application. Umetrics Academy, Umea, Sweden, 2000.

Fängmark IE, Hammarström LG, Strömquist ME, Ness AL., Norman PR, Osmond NM. Estimation of activated carbon adsorption efficiency for organic vapors. I. A strategy for selecting test compounds. *Carbon* 40:2861-9. 2002.

Freundlich H. *Colloid and Capillary Chemistry*. Methuen, London, P.120. 1926.

Furuya EG, Chang HT, Miura Y, Noll KE. *Separation and Purification Technology* 11:69-78. 1997.

Hackskaylo JJ and Levan MD. Correlation of adsorption equilibrium data using a modified Antonie equation: a new approach for pore-filling models. *Langmuir* 1:97-100. 1985.

Howard PH, Meylan WM, Handbook of physical properties of organic chemicals, CRC Press Inc., Lewis publishers, 1997.

Jakubov TS, Bering BP, Serpinski VV. Osmotic theory of gas mixtures adsorption.2. General equation of gas mixtures adsorption isotherm. *Izv. Akad. Nauk SSSR. Ser. Khim.* 991-6. 1977.

References

Jonas LA, Svirbely WJ. The kinetics of adsorption of carbon tetrachloride and chloroform from air mixtures by activated carbon. *J of Catalysis* 24:446-459. 1972.

Jonas LA, Rehrmann JA. The rate of gas adsorption by activated carbon. *Carbon* 12:95-101. 1974.

Jonas LA, Sansone EB and Farris TS. Prediction of activated carbon performance for binary vapor mixtures. *Am Ind Hyg Assoc J* 44:716-9. 1983.

Kaneko K. In: *Equilibria and Dynamics of Gas Adsorption on Heterogeneous Solid Surfaces* (Rudinski W, Steele WA and Zgrablich G, editors). Elsevier, Amsterdam, p 679. 1997.

Kenny MB, Sing KSW, Theocharis C. In: *Proc. 4th Int. Conf. On Fundamentals of Adsorption* (Suzuki M, editor), Kodansha, Tokyo, p 323. 1993.

Klotz M. The adsorption wave. *Chem Rev* 39:241-68. 1946.

Lambiotte A. Process of continuous carbonation of cellulosic materials. US patent #2,289,917, 1942.

Langmuir I. *J Am Chem Soc* 38:2221. 1916

Langmuir I. *J Am Chem Soc* 40:1361. 1918

Lavanchy A, Stokli M, Wirz C, Stoeckli F. Binary adsorption of vapors in active carbons described by the Dubinin equation. *Adsorption Sci Technol* 13:537-45. 1996.

Lavanchy A, Stoeckli F. Dynamic adsorption of vapor mixtures in active carbon beds described by the Myers-Prausnitz and Dubinin theories. *Carbon* 35:1573-9. 1997.

Lavanchy A, Stoeckli F. Dynamic adsorption, in active carbon beds, of vapor mixtures corresponding to miscible and immiscible liquids. *Carbon* 37: 315-21. 1999.

Lide DR. *Handbook of organic solvents*, CRC Press Inc. 1995.

Linders MJG, van den Broeke LJP, van Bokhoven JJGM, Duisterwinkel AED, Kapteijn F, Moulijn JA. Effect of the adsorption isotherm on one and two component diffusion in activated carbon. *Carbon* 35:1415-25. 1997.

References

Linders MJG, Prediction of breakthrough curves of activated carbon based sorption systems, Ph.D. thesis of Delft University of Technology, 1999.

Lodewyckx P, Vasant EF. Influence of humidity on adsorption capacity from the Wheeler-Jonas model for prediction of breakthrough times of water immiscible organic vapors on activated carbon beds. *Am Ind Hyg Assoc J* 61:501-05. 1999.

Lodewyckx P, Vasant EF. The influence of humidity on the overall mass transfer coefficient of the Wheeler-Jonas equation. *Am Ind Hyg Assoc J* 61:461-8. 2000.

Lodewyckx P, Vasant EF. Estimating the overall mass transfer coefficient k_v of the Wheeler-Jonas equation: a new and simple model. *Am Ind Hyg Assoc J* 61:501-05. 2000.

Lodewyckx P, Wood GO and Ryus SK. The wheeler-Jonas equation: a versatile tool for the prediction of carbon bed breakthrough times. *Carbon03*, Spain. 2003.

Mattson JS and Mark HB, Jr. *Activated carbon*. New York: Dekker. 1971.

Miller KJ and Savchik JA. A new empirical model to calculate average molecular polarizabilities. *J Am Chem Soc* 101: 7206-13. 1979.

Myers AL, Prausnitz JM. Thermodynamics of mixed gas adsorption. *AIChEJ* 11:121. 1965.

Myers AL. Adsorption of gas mixtures: a thermodynamic approach. *Ind Eng Chem.* 60:45-49. 1968.

Myers AL. Thermodynamics of adsorption in porous materials, *AIChEJ* 48:145-160. 2002.

National Institute for Occupational Safety and Health. Development of improved respirator cartridge and canister test methods by DM Smoot, Bendix Corp. Cincinnati, Ohio: Department of Health Education and Welfare; National Institute for Occupational Safety and Health, p60. 1977.

Nelson GO, Harder CA. Respirator cartridge efficiency studies:V. effect of solvent vapor. *Am Ind Hyg Assoc J* 35:391-410. 1974.

Nguyen C, Do DD. The Dubinin-Radushkevich equation and the underlying microscopic adsorption discription. *Carbon* 39:1327-36. 2001.

References

Nieszporek K. On the correct use of the Dubinin-Astakhov equation to study the mixed-gas adsorption equilibria. *Adsorption* 8:45-57. 2002.

Nir I, Suzin Y, Kaplan D. The effect of airflow pattern on filter breakthrough in physical adsorption. *Carbon* 40: 2437-45. 2002.

Noll KE, Wang D and Shen T. *Carbon* 27: 239. 1989.

O'Brien JA, Myers AL. Rapid calculations of multicomponent adsorption equilibria from pure isotherm data. *Ind Eng Chem Process Des Dev* 24:1188-91. 1985.

Oskouie AK, Miura Y, Furuya EG, Noll KE. Relationship between the highest occupied molecular orbital (HOMO) electron density of adsorption sites on carbon and the Freundlich exponent. *Carbon* 40:1199-1202. 2002.

Prakash J, Nirmalakhandan N, Speece RE. Prediction of activated carbon adsorption isotherms for organic vapors. *Environ Sci Technol* 28:1403-9. 1994.

Reucroft PJ, Simpson WH, Jonas LA. Sorption properties of activated carbon. The *Journal of Physical chemistry* 75(23):3526-31. 1971.

Richter E, Schutz W, Myers AL. Effect of adsorption equation on prediction of multicomponent adsorption equilibria by the ideal adsorbed solution theory. *Chemical Engineering Science* 44:1609-16. 1989.

Riddick JA, Bunger WB, Sakano TK. Organic solvents: physical properties and methods of purification, 4th Ed. Techniques of chemistry Vol.II, Ser.Ed. Weissberger A. Wiley-Interscience, 1986.

Robbins CA and Breysse PN. The effect of vapor polarity and boiling point on breakthrough for binary mixtures on respirator carbon. *Am Ind Hyg Assoc J* 57:717-23. 1996.

Rodriguez-Reinoso F and A Linares-Solano. *Chemistry and physics of carbon: a series of advances* (P.A.Thrower, Ed.), Marcel Dekker, Inc., New York. 1989.

Roplex Engineering Ltd. Roplex House, Church Road, Shedfield, Hants. SO32 2HW

Ruthven DM, Loughlin KF, Holbarow KA. Multicomponent sorption equilibrium in molecular sieve zeolites. *Chem Eng Sci* 28:701-9. 1973.

References

Ruthven DM. Sorption of oxygen, nitrogen, carbon monoxide, methane, and binary mixtures of these gases in 5A molecular sieve. *AIChE J* 22:753-9.1976.

Sing KSW. In: Characterization of porous solids (Gregg SJ, Sing KSW, Stoeckli HF editors.), Society of Chemical Industry, London, p 98. 1979.

Sing KSW, Everett DH, Haul RAW, Moscou L, Pierotti RA, Rouquerol J, Siemieniewska T. Reporting physisorption data for gas/solid systems with special reference to the determination of surface area and porosity. *Pure & Appl Chem* 57(4):603-19. 1985.

Per Sjöberg, Molsurf version, Qemist AB, Hertig Carls alle' 29, SE-691 41 Karlskoga, Sweden. Qemist@swipnet.se

Stoeckli F. A generalization of the Dubinin-Radushkevich equation for the filling of heterogeneous micropore systems. *J Colloid Interface Sci* 59:184-5. 1977.

Stoeckli HF, Houriet JP, Perret A and Huber U. In: *Characterization of porous solids* (Gregg SJ, KSW Sing and HF Stoeckli, eds.), Society of Chemical Industry, London, p.31. 1979.

Stoeckli HF and Morel D. On the physical meaning of parameters E_0 and β IN Dubinin's theory. *Chimia* 34: 503. 1980.

Stoeckli F. Microporous carbons and their characterization: the present state of art. *Carbon* 28:1-6. 1990.

Stoeckli F. Recent developments in Dubinin's theory. *Carbon* 36:363-8. 1998.

Stoeckli F, Couderc G, Wintgens D, Lavanchy A, Girardin Ph. The non-ideality of the system 1,2-dichloethane+benzene adsorbed in microporous carbons at 293K. *Adsorption Sci & Technol* 18:581-9. 2000.

Sundaram N. Equation for adsorption from gas mixtures. *Langmuir* 11:3223-34. 1995.

Suwanayuen S, Danner RP. A gas adsorption isotherm equation based on vacancy solution theory. *AIChE J* 26:68-76. 1980.

Swearengen PM and Weaver SC. Respirator cartridge study using organic-vapor mixtures. *Am Ind Hyg Assoc J* 49:70-4. 1988.

References

Urano K, Omori S, Yamamoto E. Prediction method for adsorption capacities of commercial activated carbons in removal of organic vapors. *Environ Sci Technol* 16:10-4. 1982.

Vermeulen T, Levan MD, Hiester NK, Klein G. Adsorption and ion exchange. In: Perry RH et al., editor, *Perry's chemical engineers handbook*, 6th ed., New York: McGraw Hill, p1-48. 1984.

Vahdat N, Swearengen PM and Johnson JS. Adsorption prediction of binary mixtures on adsorbents used in respirator cartridges and air-sampling monitors. *Am Ind Hyg Assoc J* 55:909-17. 1994.

Wheeler A, Robell AJ. Performance of fixed-bed catalytic reactors with poison in the feed. *J Catal* 13:299-305. 1969.

Wold S, Albano C, Dunn III WJ, Edlund U, Esbensen P, Geladi P, Hellberg E, Lindberg W, Sjostrom M. In: *Chemometrics-Mathematics and Statistics in Chemistry*. Kowalski BR, Ed. Riedel Publ. Co: Dordrect, p17-95. 1984

Wold S. Validation of QSARs. *Quant Struct Act Relat* 10:191-3. 1991.

Wood GO, Moyer ES. A review of the Wheeler equation and comparison of its application to organic vapor respirator cartridge breakthrough data. *Am Ind Hyg Assoc J* 50:400-7. 1989.

Wood GO, Moyer ES. A review and comparison of adsorption isotherm equations used to correlate and predict organic vapor cartridge capacities. *Am Ind Hyg Assoc J* 52:235-42. 1991.

Wood GO. Activated carbon adsorption capacities for vapors. *Carbon* 30:593-9. 1992.

Wood GO, Stampfer JF. Adsorption rate coefficients for gases and vapors on activated carbons. *Carbon* 31:195-200. 1993.

Wood GO. Affinity coefficients of the polanyi/Dubinin adsorption isotherm equations. *Carbon* 39:343-56. 2001.

Wood GO. Review and comparison of D/R models of equilibrium adsorption of binary mixtures of organic vapors on activated carbons. *Carbon* 40:231-9. 2002.

References

Wood GO. A review of the effects of covapors on adsorption rate coefficients of organic vapors adsorbed onto activated carbon from flowing gases. *Carbon* 40:685-94. 2002.

Wood GO. Quantification and application of skew of breakthrough curves for gases and vapors eluting from activated carbon beds. *Carbon* 40:1883-90. 2002.

Wood GO and Lodewyckx P. Anextended equation for rate coefficients for adsorption of organic vapors and gases on activated carbons in air-purifying respirator cartridges. *Am Ind Hyg Assoc J* 64:646-50. 2003.

Yoon YH and Nelson JH. Application of gas adsorption kinetics: I. A theoretical model for respirator cartridges service life. *Am Ind Hyg Assoc J* 45:509-16. 1984.

Yoon YH and Nelson JH. Application of gas adsorption kinetics: II. A theoretical model for respirator cartridges service life and its practical application. *Am Ind Hyg Assoc J* 45:517-24. 1984.

Yoon YH, Nelson JH, Lara J, Kamel C and Fregeau D. A theoretical interpretation of the service life of respirator cartridges for the binary acetone/m-xylene system. *Am Ind Hyg Assoc J* 52:65-74. 1991.

Yoon YH, Nelson JH, Lara J, Kamel C and Fregeau D. A theoretical model for respirator cartridge service life for binary systems: application to acetone/styrene mixtures. *Am Ind Hyg Assoc J* 53:493-502. 1992.

Appendix I

APPENDIX I: A list of 68 organic compounds

Id#	Compound	Id#	Compound	Id#	Compound
1	1,4-Dioxane	29	Butane	59	Chloroform
2	Fluorobenzene	31	Chloropicrin	60	1,1,1-Trichloroethane
3	Formic acid	32	Diethylether	61	Trichloroethylene
4	Neopentane	33	Isopropylamine	62	1,1,2-Trichloroethane
6	Nitromethane	34	Propylamine	64	Carbon tetrachloride
10	Propionaldehyde	35	Diethylamine	68	2-Butanone
13	Benzene	36	Butylamine	69	2-Pentanone
14	Toluene	37	Triethylamine	70	4-Methyl-2-pentanone
15	Methanol	38	Dipropylamine	76	Methylamine
16	Ethanol	39	Diisopropylamine	77	Dimethylamine
17	2-Propanol	40	Cyclohexylamine	78	Ethylamine
18	1-Butanol	44	Chloroethane	79	Carbon disulfide
19	Acetaldehyde	45	2-Chloropropane	80	Acetone
20	Methyl acetate	46	3-Chloropropene	81	1,2-Dichloroethane
21	Ethyl acetate	47	1-Chloropropane	83	Allylamine
22	Acetonitrile	48	2-Chloro-2-methylpropane	85	Diallylamine
23	Pentane	49	1-Chlorobutane	87	3-Pentanone
24	Hexane	50	1-Chloropentane	88	2,2-Difluoropropane
25	Cyclohexane	53	Dichloromethane	89	N,N-Dimethylethylamine
26	2,2,4-Trimethylpentane	54	trans-1,2-Dichloroethylene	91	Acrolein
27	Heptane	55	1,1-Dichloroethane	92	1-Bromopropane
28	Pyridine	56	cis-1,2-Dichloroethylene	93	2-Bromopropane
		57	1,2-Dichloropropane	95	Bromomethane

Appendix II

APPENDIX II: Breakthrough curves of single compounds on Norit R1, AR1 and AR2.

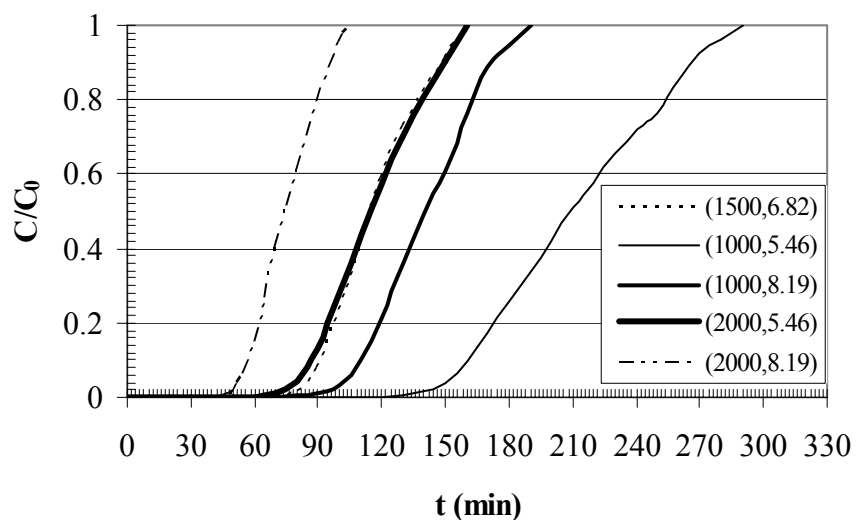


Fig.1. Breakthrough curves of benzene on Norit R1.

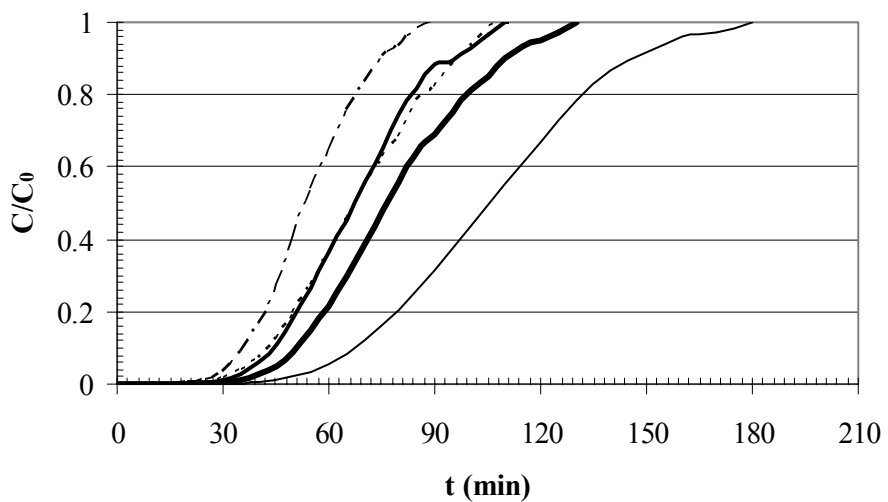


Fig.2. Breakthrough curves of acetonitrile on Norit R1.

Appendix II

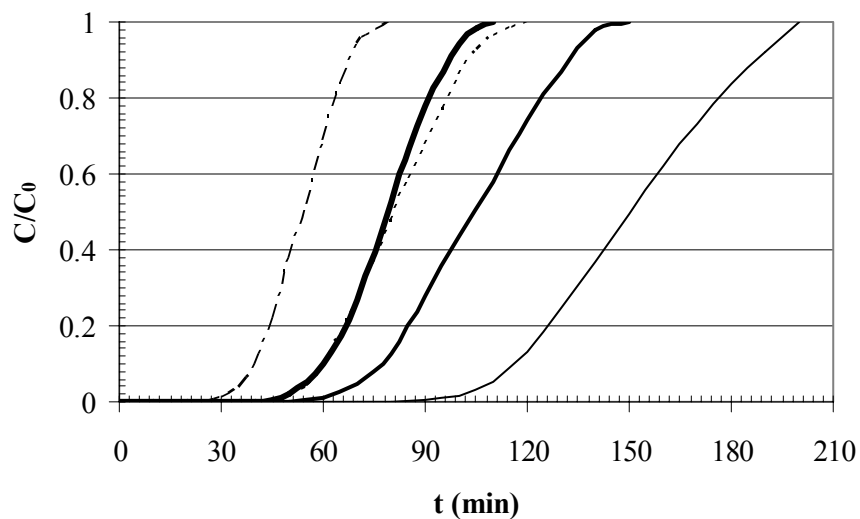


Fig.3. Breakthrough curves of heptane on Norit R1.

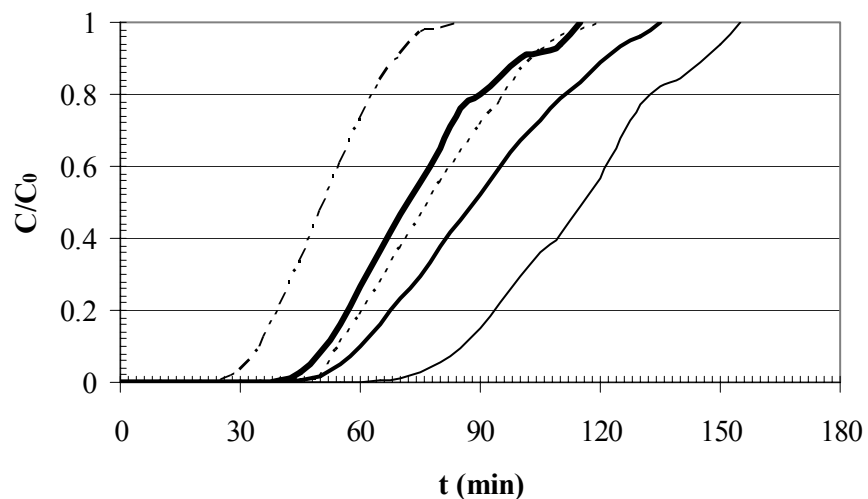


Fig.4. Breakthrough curves of isopropylamine on Norit R1.

Appendix II

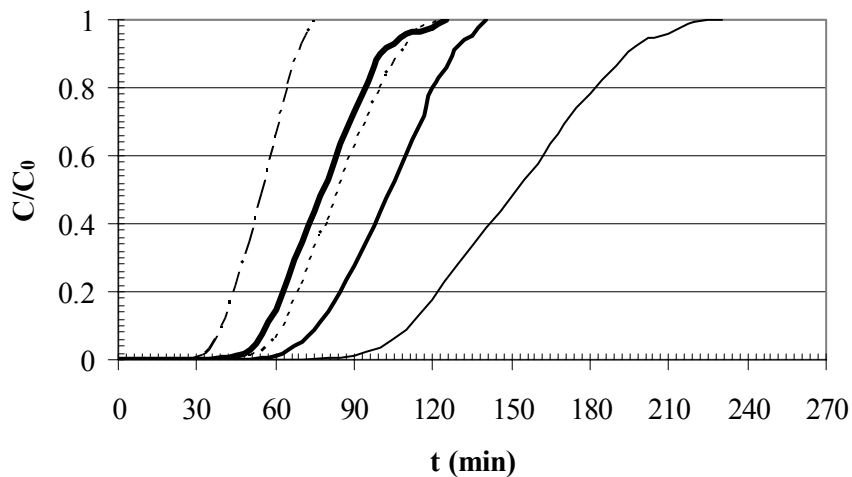


Fig.5. Breakthrough curves of 2-chloro-2-methyl-propane on Norit R1.

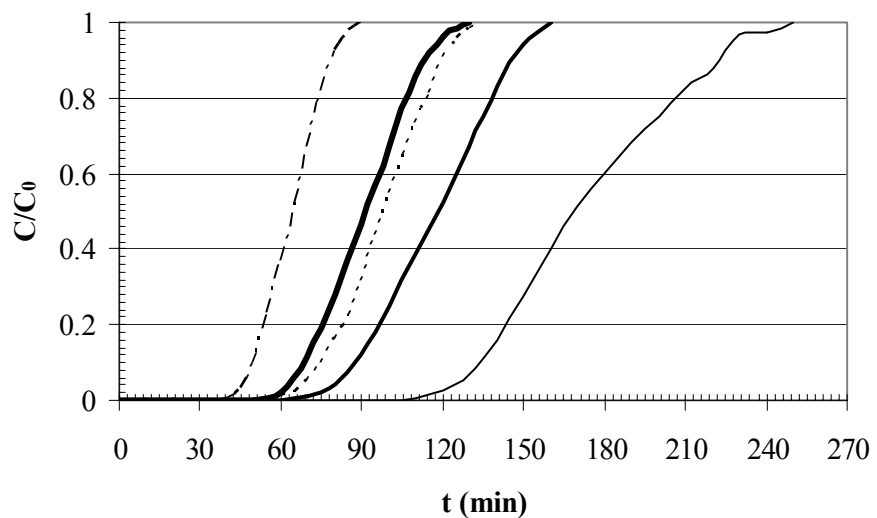


Fig.6. Breakthrough curves of chloropentane on Norit R1.

Appendix II

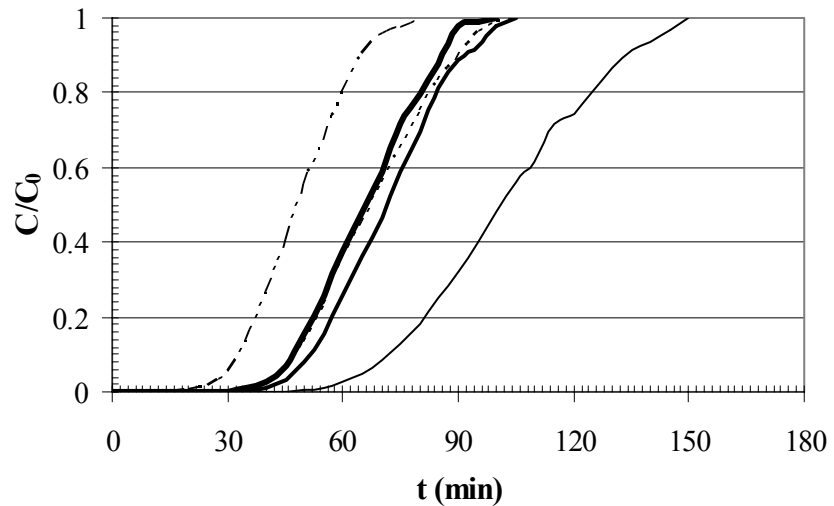


Fig.7. Breakthrough curves of dichloromethane on Norit R1.

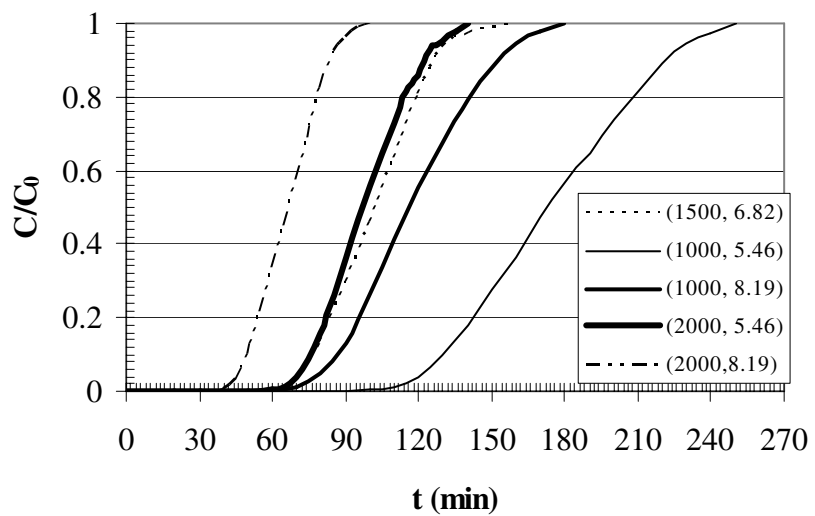


Fig.8. Breakthrough curves of 2-butanone on Norit R1.

Appendix II

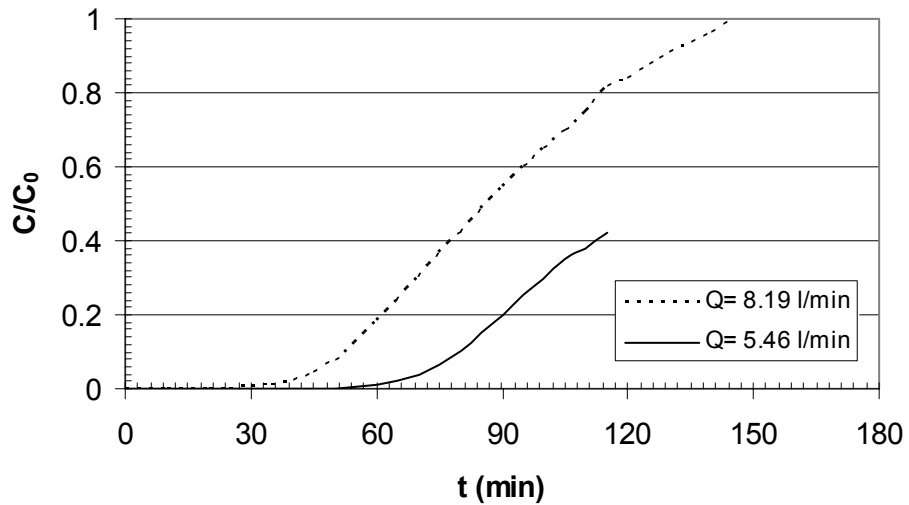


Fig.9. Breakthrough curves of propionaldehyde on AR1 ($C_0 = 1000 \text{ ppm}$).

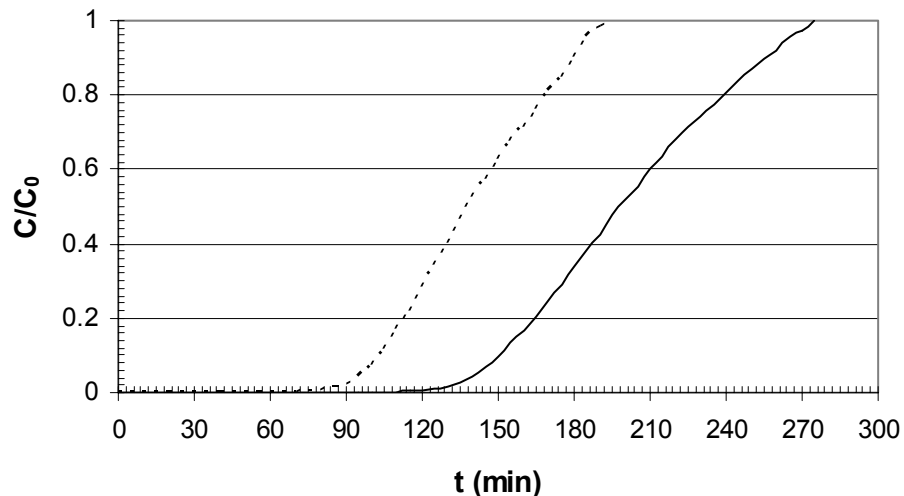


Fig.10. Breakthrough curves of benzene on AR1 ($C_0 = 1000 \text{ ppm}$).

Appendix II

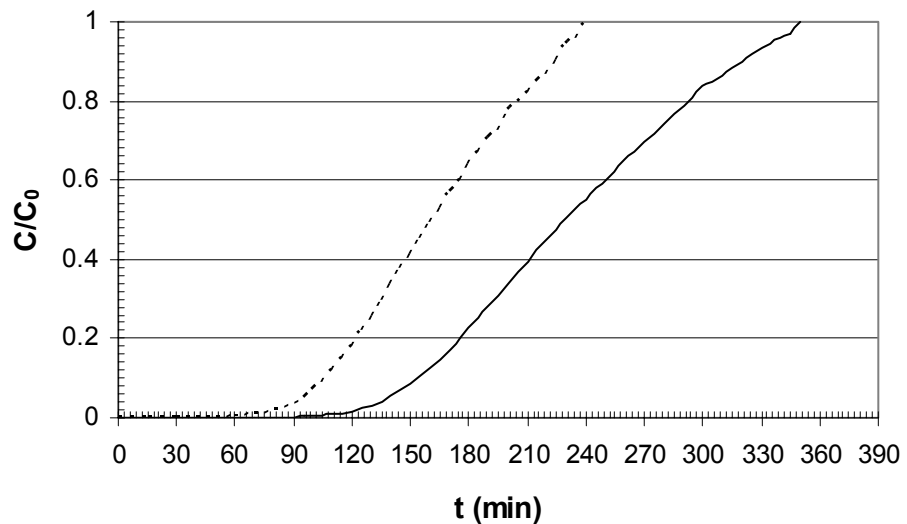


Fig.11. Breakthrough curves of 2-propanol on AR1 ($C_0 = 1000$ ppm).

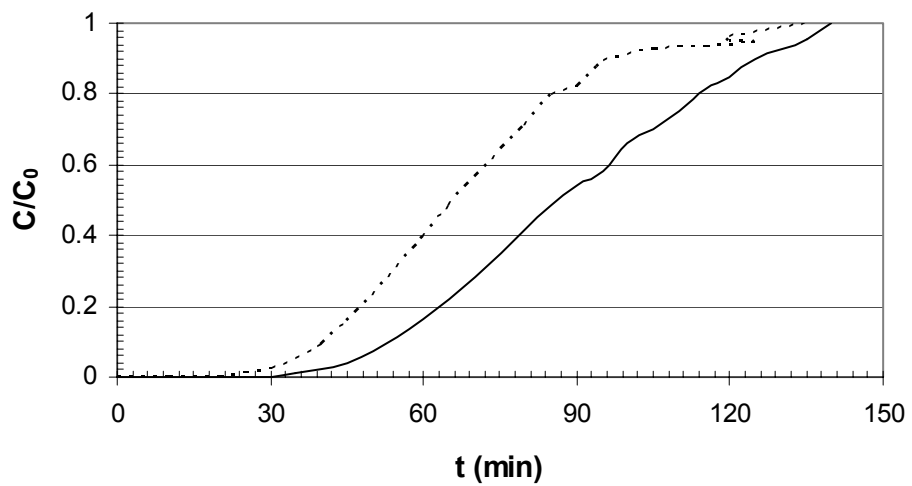


Fig.12. Breakthrough curves of acetonitrile on AR1 ($C_0 = 1000$ ppm).

Appendix II

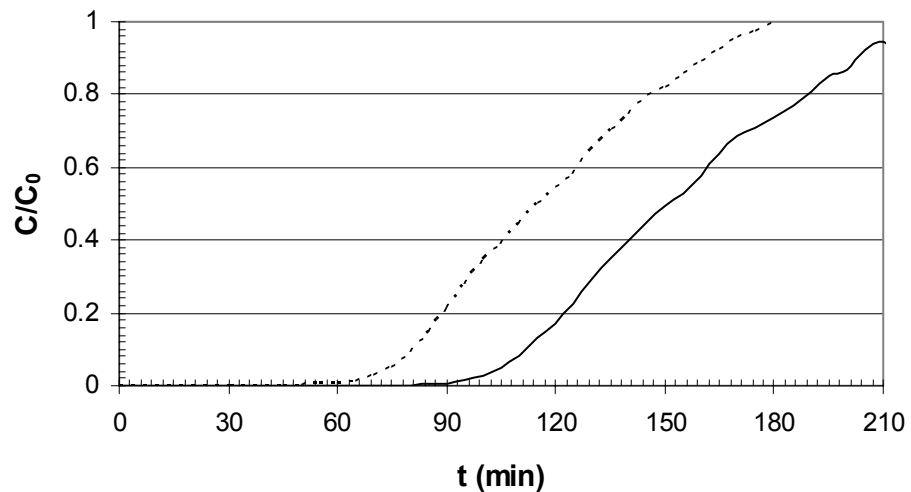


Fig.13. Breakthrough curves of 2,2,4-trimethylpentane on AR1 ($C_0 = 1000$ ppm.).

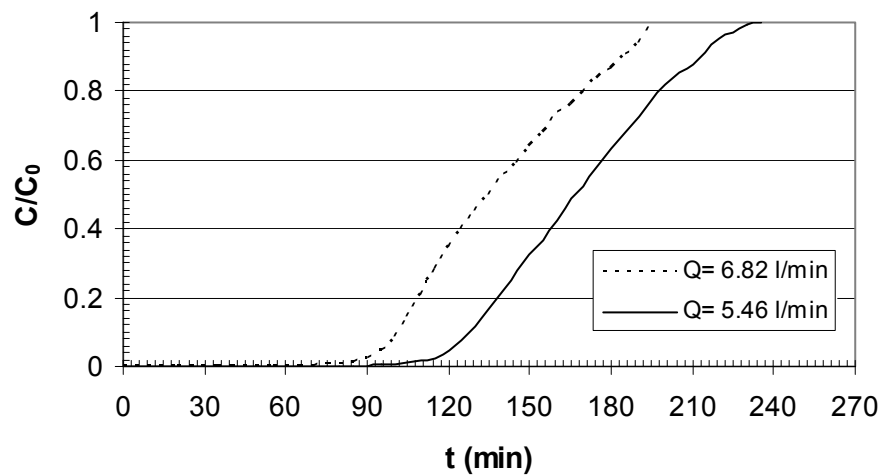


Fig.14. Breakthrough curves of heptane on AR1 ($C_0 = 1000$ ppm).

Appendix II

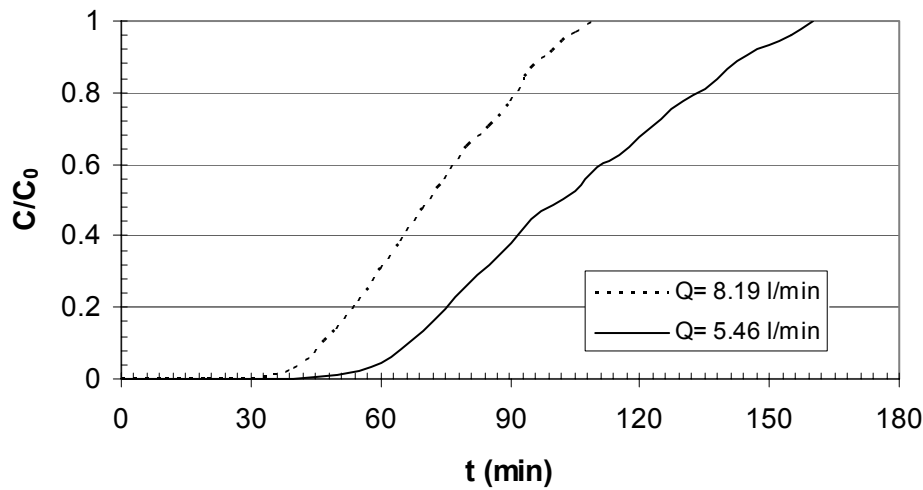


Fig.15. Breakthrough curves of isopropylamine on AR1 ($C_0 = 1000$ ppm).

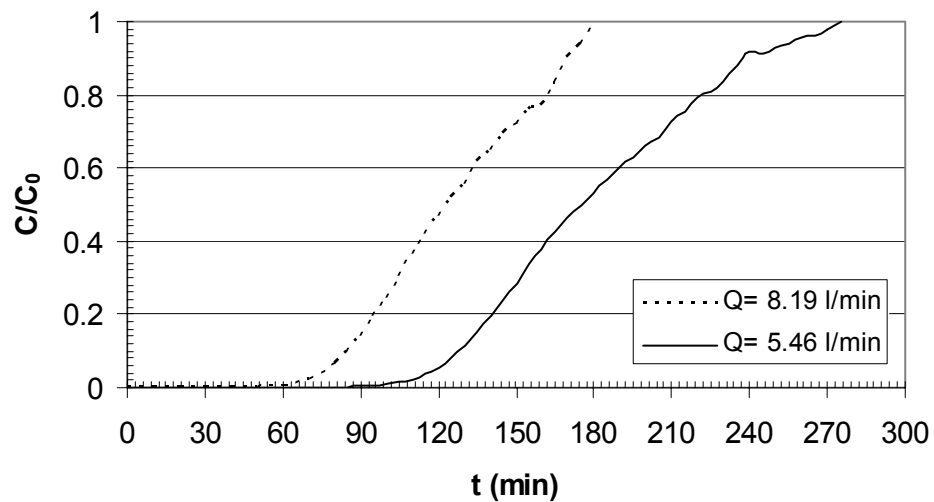


Fig.16. Breakthrough curves of 1,1,1-trichloroethane on AR1 ($C_0 = 1000$ ppm).

Appendix II

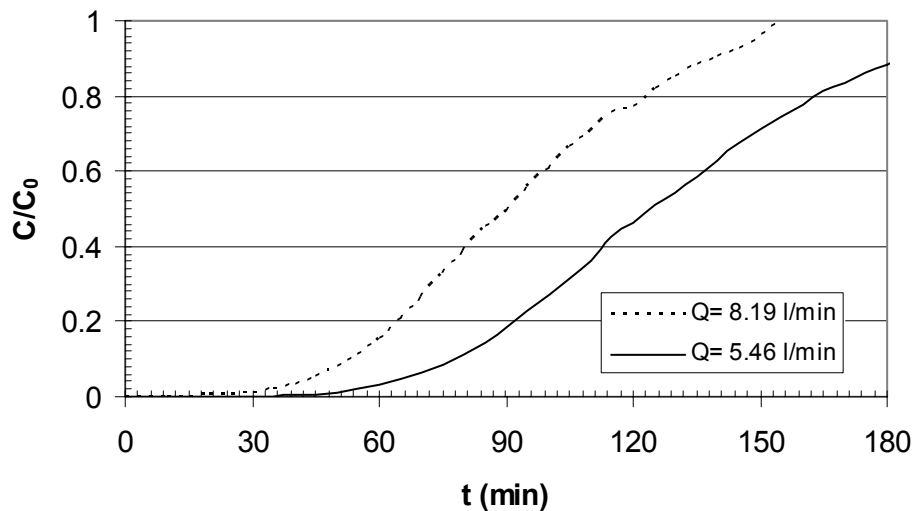


Fig.17. Breakthrough curves of propionaldehyde on AR2 ($C_0 = 1000$ ppm).

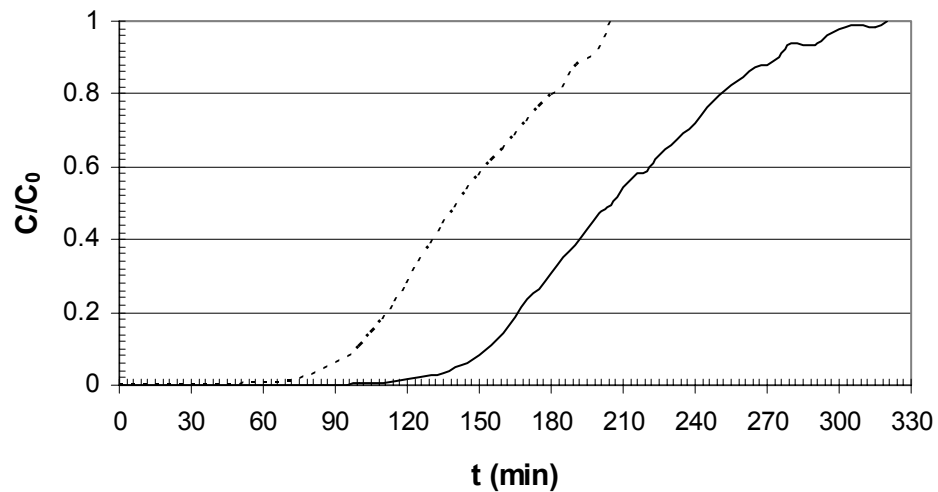


Fig.18. Breakthrough curves of benzene on AR2 ($C_0 = 1000$ ppm).

Appendix II

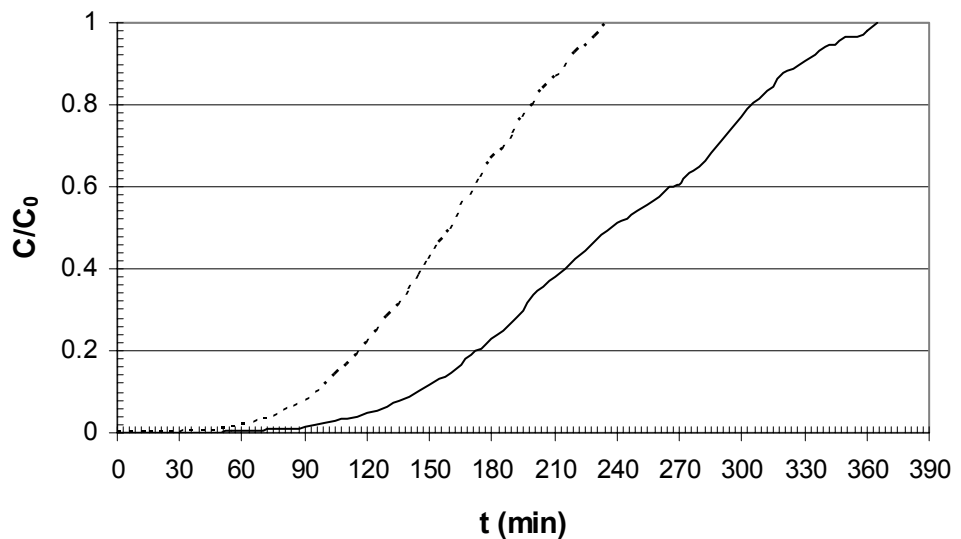


Fig.19. Breakthrough curves of 2-propanol on AR2 ($C_0 = 1000$ ppm).

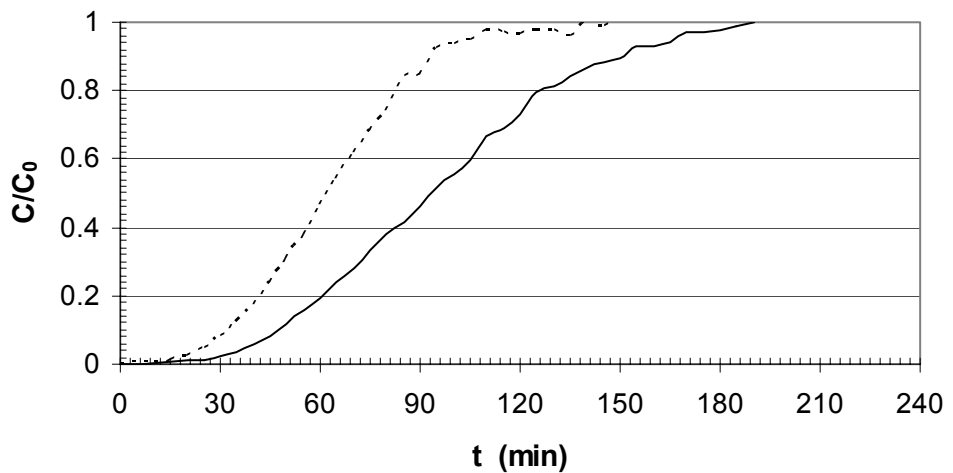


Fig.20. Breakthrough curves of acetonitrile on AR2 ($C_0 = 1000$ ppm).

Appendix II

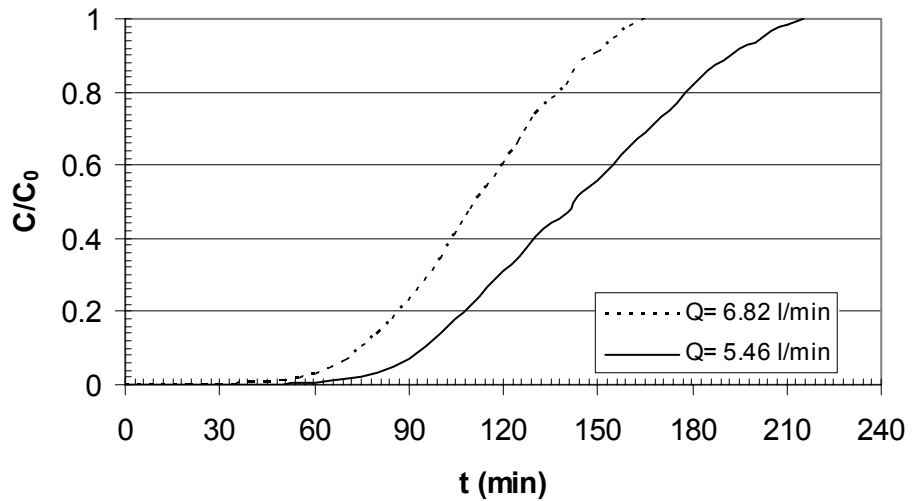


Fig.21. Breakthrough curves of 2,2,4-trimethylpentane on AR2 ($C_0 = 1000 \text{ ppm}$).

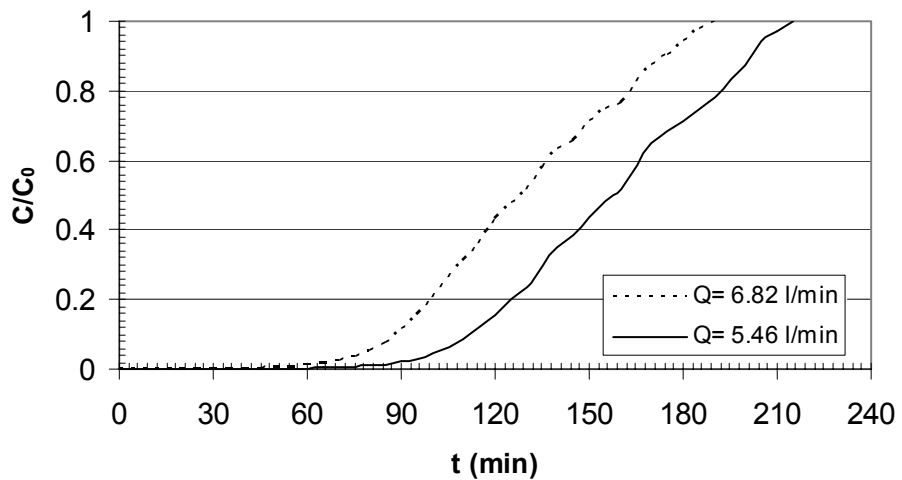


Fig.22. Breakthrough curves of heptane on AR2 ($C_0 = 1000 \text{ ppm}$).

Appendix II

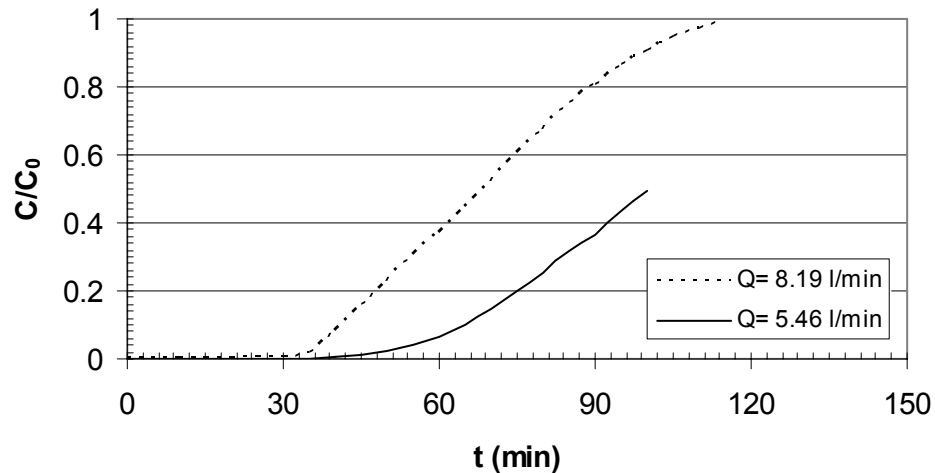


Fig.23. Breakthrough curves of isopropylamine on AR2 ($C_0 = 1000 \text{ ppm}$).

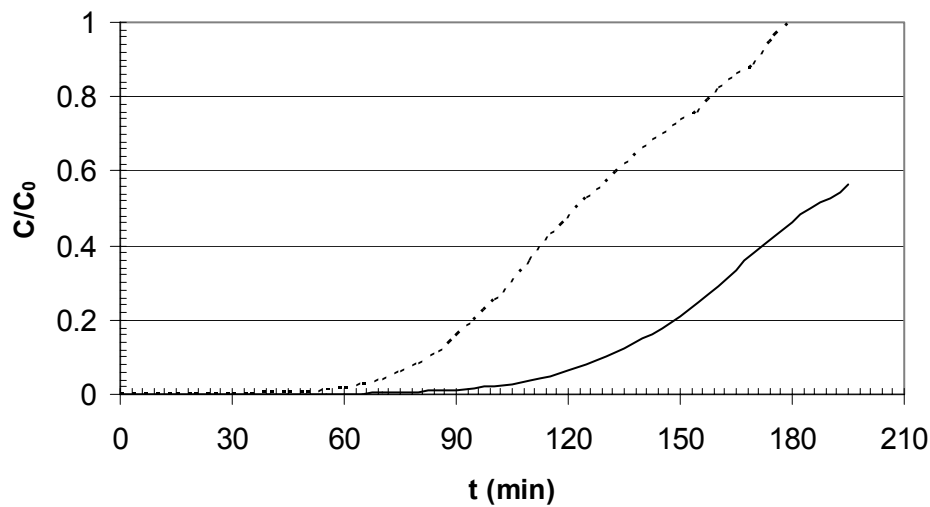


Fig.24. Breakthrough curves of 1,1,1-trichloroethane on AR2 ($C_0 = 1000 \text{ ppm}$).

Appendix III

APPENDIX III: Breakthrough curves of binary mixtures on Norit R1.

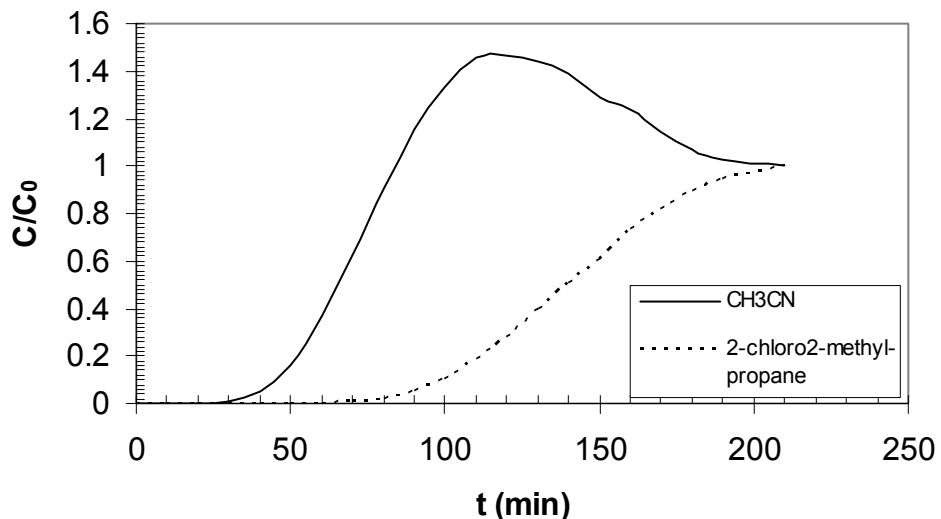


Fig.1. Breakthrough curves of 22-48 ($C_0 = 1000$ ppm, $Q = 5.46$ l/min).

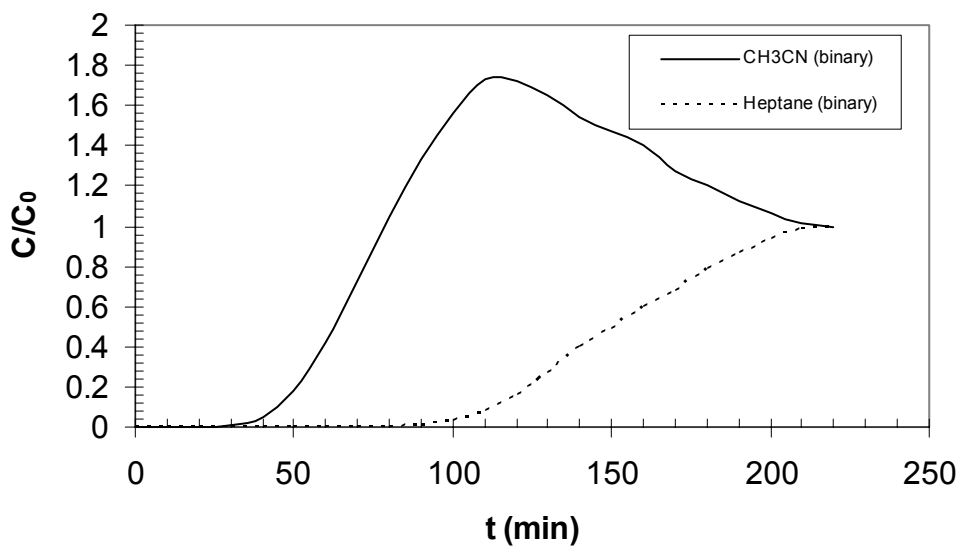


Fig.2. Breakthrough curves of 22-27 ($C_0 = 1000$ ppm, $Q = 5.46$ l/min).

Appendix III

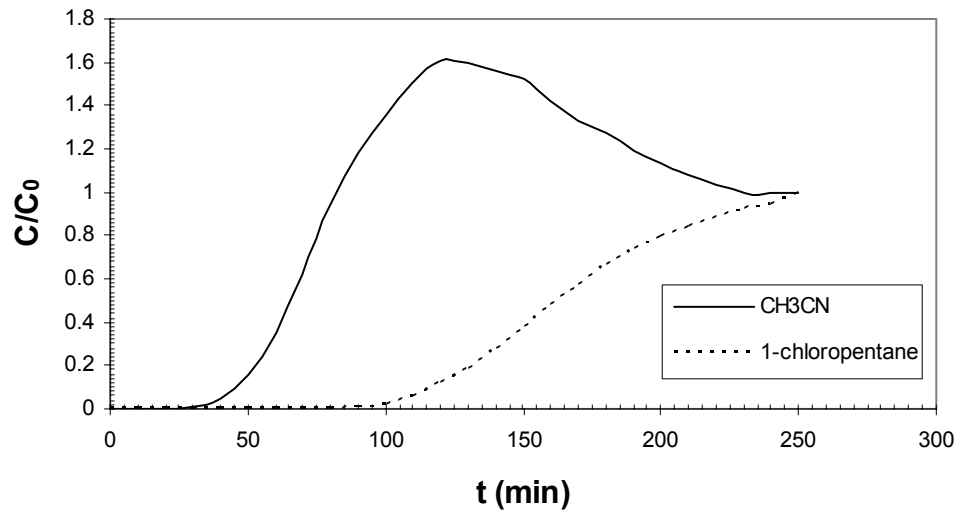


Fig.3. Breakthrough curves of 22-50 ($C_0 = 1000$ ppm, $Q = 5.46$ l/min).

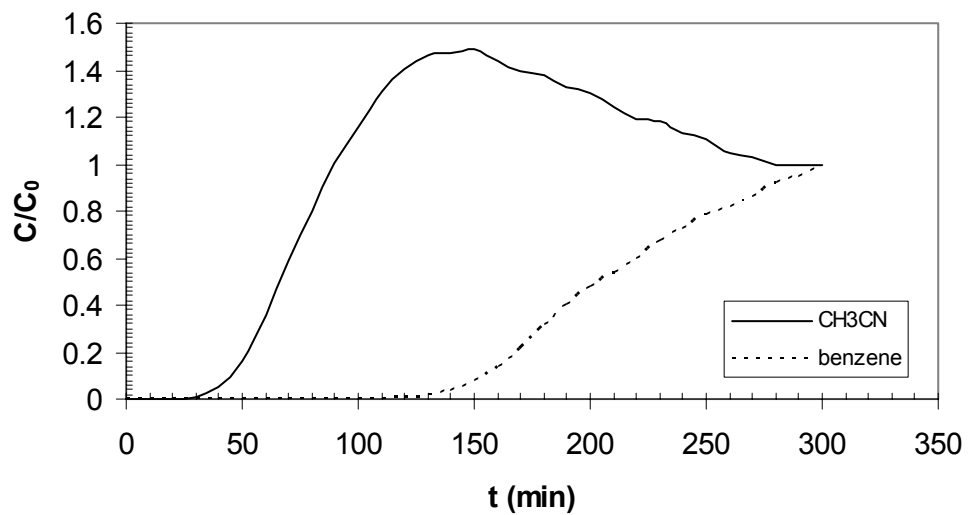


Fig.4. Breakthrough curves of 22-13 ($C_0 = 1000$ ppm, $Q = 5.46$ l/min).

Appendix III

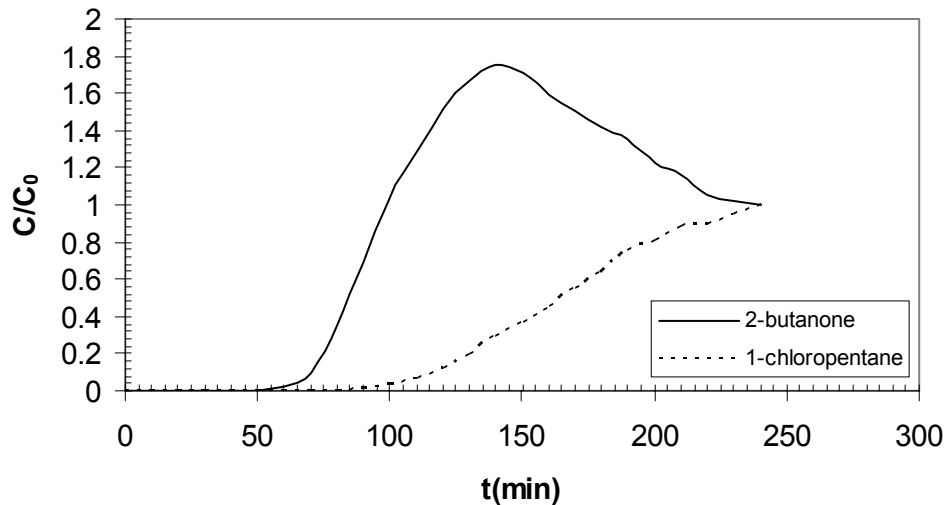


Fig.5. Breakthrough curves of 68-50 ($C_0 = 1000$ ppm, $Q = 5.46$ l/min).

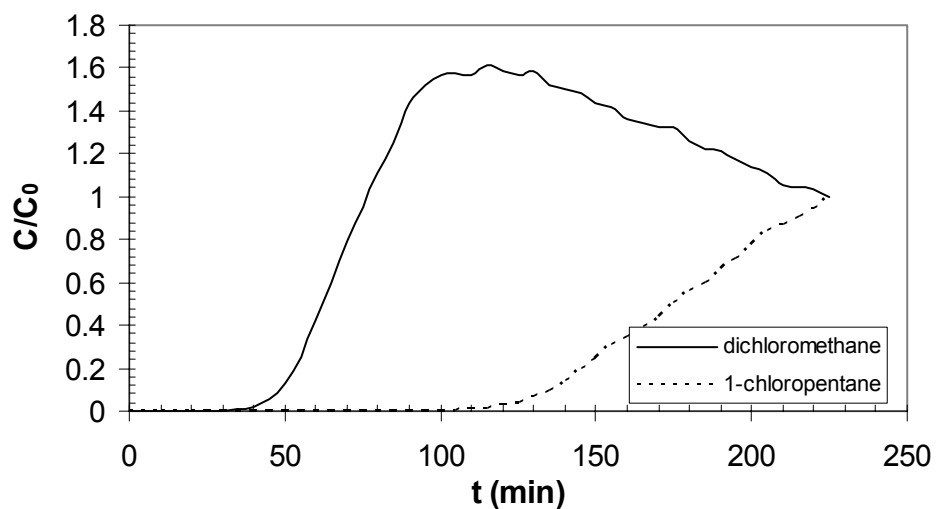


Fig.6. Breakthrough curves of 53-50 ($C_0 = 1000$ ppm, $Q = 5.46$ l/min).

Appendix III

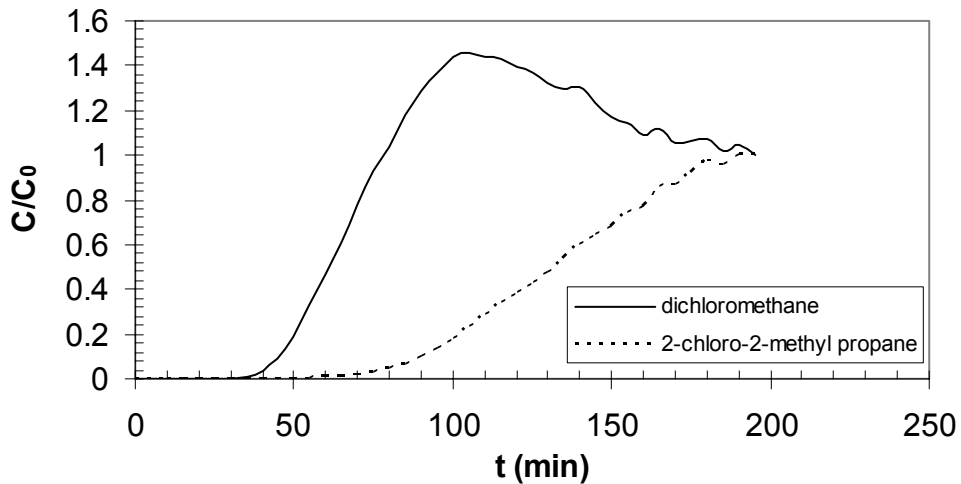


Fig.7. Breakthrough curves of 53-48 ($C_0 = 1000$ ppm, $Q = 5.46$ l/min).

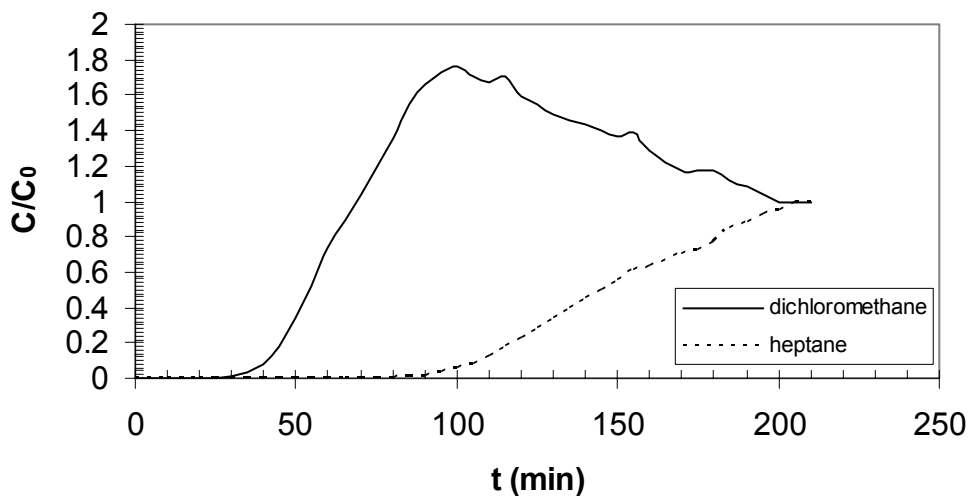


Fig.8. Breakthrough curves of 53-27 ($C_0 = 1000$ ppm, $Q = 5.46$ l/min).

Appendix III

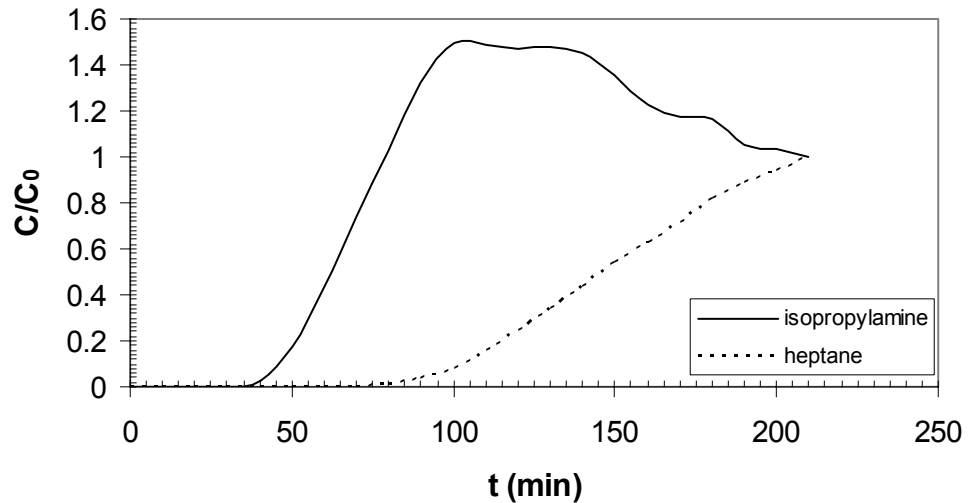


Fig.9. Breakthrough curves of 33-27 ($C_0 = 1000$ ppm, $Q = 5.46$ l/min).

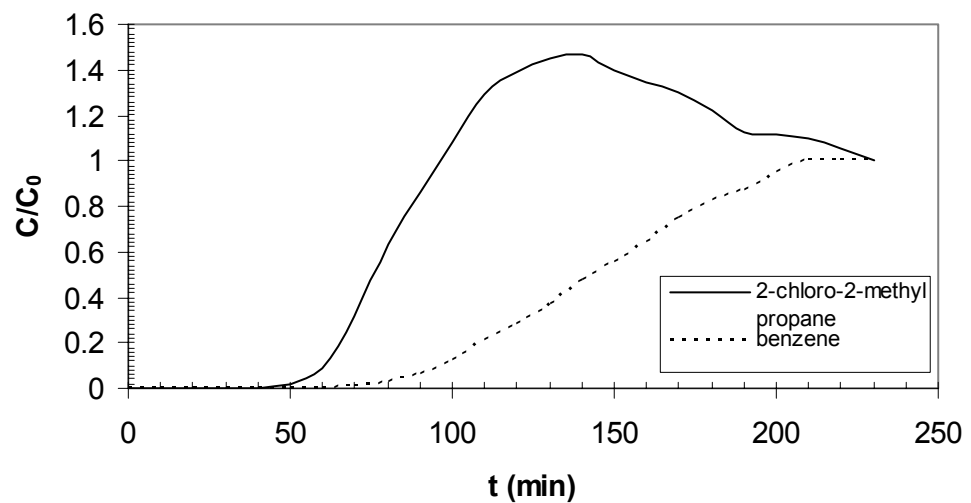


Fig.10. Breakthrough curves of 48-13 ($C_0 = 1000$ ppm, $Q = 5.46$ l/min)

Appendix III

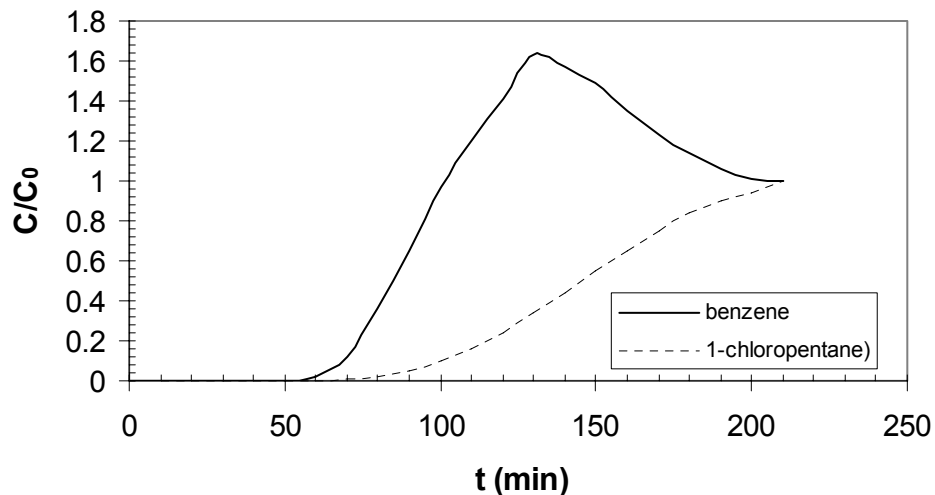


Fig.11. Breakthrough curves of 13-50 ($C_0 = 1000$ ppm, $Q = 5.46$ l/min).